We are IntechOpen, the world's leading publisher of Open Access books Built by scientists, for scientists

4,800
Open access books available

122,000
International authors and editors

135M
Downloads

Our authors are among the

154
Countries delivered to

TOP 1%
most cited scientists

12.2%
Contributors from top 500 universities

CLARIVATE ANALYTICS BOOK CITATION INDEX INDEXED

WEB OF SCIENCE™

Selection of our books indexed in the Book Citation Index in Web of Science™ Core Collection (BKCI)

Interested in publishing with us?
Contact book.department@intechopen.com

Numbers displayed above are based on latest data collected.
For more information visit www.intechopen.com

24

Liquid crystal dispersions of carbon nanotubes: dielectric, electro-optical and structural peculiarities

L. Dolgov[1*], O. Koval'chuk[2], N. Lebovka[3], S. Tomylko[2,4], and O. Yaroshchuk[2]
[1]*Institute of Physics, University of Tartu, 51014 Tartu, Estonia*
[2]*Institute of physics, NASU, prospekt Nauki 46, 03028 Kyiv, Ukraine*
[3]*Institute of Biocolloidal Chemistry, NASU, Vernadskii Prosp. 42, 03142 Kyiv, Ukraine*
[4]*Taras Shevchenko National University, Physical Faculty, prospekt Glushkova 2, 03022 Kyiv, Ukraine*

1. Introduction

Liquid crystals (LCs) turn out to be excellent hosts for carbon nanotubes (CNTs). Having molecular structure similar to CNTs, LCs perfectly incorporate CNTs into own structure. Particularly, the liquid crystalline orientational order can be imposed on CNTs so that aligned ensembles of these particles can be attained (Dierking et al., 2004). This alignment can be patterned by pattering alignment of LC host. Furthermore, the alignment axis of CNTs can be easily driven by the LC reorientation in the external field (Dierking et al., 2008); CNTs follow reorientation of LC director demonstrating guest-host effect known for molecular solutions and dispersions of anisotropic nanoparticles in LC hosts (Blinov & Chigrinov, 1996). Finally, LC can be removed and thus pure aligned CNTs can be obtained (Lynch & Patrick, 2002). This altogether means that LC gives unique opportunity for controllable alignment of CNTs.

On the other hand, CNTs bring a number of improvements to LC layers used in electro-optic devices (Qi & Hegmann, 2008). The LC doping by CNTs reduces response time (Huang et al., 2005; Chen et al., 2007; Lee et al., 2008) and driving voltage (Lee et al., 2004), suppresses parasitic back flow and image sticking typical for LC cells (Lee et al., 2004; Baik et al., 2005; Chen & Lee, 2006).

The LC-CNTs systems are not limited to nematic matrices. A series of unique LC-CNTs composites based on thermotropic and lyotropic materials with different LC mesophases is developed and characterized (Weiss et al., 2006; Lagerwall et al., 2006, Lagerwall et al., 2007; Cervini et al., 2008; Podgornov et al., 2009).

A symbiosis of LC and CNTs rouses rapidly increasing interest. The number of publications on this subject grows in geometrical progression. The major results of these studies are summarized in several recent reviews (Lagerwall & Scalia, 2008; Rahman & Lee, 2009).

---

[*] on leave of absence from *Institute of physics, NASU, prospect Nauki 46, 03028 Kyiv, Ukraine*

A present chapter is focused on remarkable dielectric, electro-optical and micro-structural peculiarities of LC-CNTs dispersions, their correlation and mutual influence. It is mainly based on authors' original results obtained within recent years. The structure of this chapter is the following. The introductory part (section 1) gives short introduction to LC-CNTs composites and elucidates benefit of combination of LC and CNTs. It also outlines a field of questions further considered. A section 2 gives details of our samples and experimental methods. The next three sections correspondingly consider dielectric, electro-optical and structural peculiarities of LC-CNTs composites. Each of these topical sections starts with a short review and lasts with the authors' original results. The final, conclusion part (Section 6), summarizes most interesting properties of LC-CNTs suspensions, their application perspectives and mention some exciting problems for further investigations.

2. Materials and methods

2.1 Liquid crystalline media and chiral dopant

Nematic LCs EBBA (Reakhim, Russia), 5CB, MLC6608, and MLC6609 (Merck, Germany) were used as LC hosts. EBBA was purified by fractional crystallization from the n-hexane solution, 5CB, MLC6608, MLC6609 were used as obtained. Some characteristics of these LCs are presented in Table 1.

LC	Nematic mesophase	dielectric anisotropy $\Delta\varepsilon$, optical anisotropy Δn	Reference
EBBA	308.9 - 350.6 K	$\Delta\varepsilon$=-0.13, Δn=0.25 at 313 K	Goncharuk et al., 2009
5CB	295.5- 308.3 K	$\Delta\varepsilon$=13, Δn=0.177 at 298 K	Blinov & Chigrinov, 1996
MLC6608	clearing point at 363 K	$\Delta\varepsilon$=-4.2, Δn=0.0830 at 293 K	Licristal®, 2002
MLC6609	clearing point at 364.5 K	$\Delta\varepsilon$=-3.7, Δn=0.0777 at 293 K	Licristal®, 2002

Table 1. Characteristics of LC media.

S811 (Merck, Germany) was used as chiral dopant.

2.2 Multiwalled carbon nanotubes

The multiwalled carbon nanotubes (SpetsMash Ltd., Ukraine) were prepared from ethylene by the chemical vapor deposition method (Melezhyk et. al., 2005). Typically, these CNTs have an outer diameter of about 12–20 nm and the length of about 5-10 μm. The specific electric conductivity σ of the powder of compressed CNTs was about 10^3 S/m along the compression axis.

2.3 Preparation of LC-CNTs composites

The all LC-CNTs composites were prepared by 20 min stirring of LC and CNT mixtures using the ultrasonic mixer equipped with a cup horn, at the frequency of 22 kHz and the output

power of 150 W. The concentration of CNTs, *c*, was varied in the range 0-2 wt %. Doping of CNTs has not influenced essentially the phase transition temperatures of LC-CNTs composites.

2.4 Cells

The cells for electro-optical and dielectric measurements were made from glass substrates containing patterned ITO electrodes and aligning layers of polyimide. The polyimides AL2021 (JSR, Japan) and SE5300 (Nissan Chemicals, Japan) were used for homeotropic alignment of LC EBBA, MLC6608 and MLC6609, while the polyimide SE150 (Nissan Chemicals, Japan) was utilized for planar alignment of LC 5CB. The polyimide layers were rubbed by a fleecy cloth in order to provide a uniform planar alignment of LC in either field-on state (EBBA, MLC6608 and MLC6609) or a zero field (5CB). The cells were assembled so that the rubbing directions of the opposite aligning layers were antiparallel. A cell gap was maintained by the glass spacers of appropriate size (16 μm, if not otherwise stated). Finally, these cells were filled capillary with neat or CNTs doped liquid crystals heated to isotropic state. In some dielectric measurements the cells without alignment layers were utilized. The structure of LC-CNTs composites was monitored by observation of the filled cells placed between crossed polarizers, both by naked eye and in an optical polarizing microscope.

2.5 Electro-optical measurements

The electro-optical measurements were carried out using the experimental setup described in (Koval'chuk et al., 2001a). The cell was set between two crossed polarizers so that the angle between the polarizer axes and the rubbing direction was 45°.

The sinusoidal voltage 0-60 V (at frequency f=2 kHz) was applied to the cell. The voltage was stepwise increased from 0 to 60 V and then decreased back to 0; the total measuring time, i.e., time of voltage application, was about 1 min. The transmittance of the samples was calculated as $\eta=(I_{out}/I_{in})*100\%$, where I_{in} and I_{out} are intensities of the incident and transmitted light, respectively.

2.6 Dielectric measurements

The dielectric spectra in the frequency region between $5\cdot10^{-2}$ and 10^6 Hz were recorded by measurement of the frequency f dependences of resistance R and capacitance C using the oscilloscopic method (Twarowski & Albrecht, 1979; Koval'chuk, 1998). The voltage signal applied to the tested cell had a triangle form with amplitude of 0.25 V. The parallel connected R-C circuit was used as an equivalent scheme of the cell and the values of the real (capacitive) ε' and imaginary (ac conductance) ε'' components of the permittivity $\varepsilon=\varepsilon'+i\varepsilon''$ of a composite were then calculated. Based on ε'' data the sample conductivity σ was determined using a formula:

$$\sigma = 2\pi\varepsilon_o\varepsilon'' f, \quad (1)$$

where ε_0 is a dielectric constant.

The ac electrical conductivity was also measured by a LCR meter 819 (Instek, 12 Hz–100 kHz) in the non-relaxation frequency range preliminarily determined from the dielectric spectra. All the measurements were repeated at least 5 times in order to calculate the average values and errors.

3. Dielectric studies of LC composites doped with carbon nanotubes

The interest to the electrophysical behavior of LC composites doped with carbon nanotubes is continuously growing (Lebovka et al., 2008; Lu & Chien, 2008; Koval'chuk et al., 2008). Dispersed nanotubes essentially influence the concentration and spatial distribution of charges in LC cells and thus determine the actual electric field applied to the composites and their electro-optic response (Lee et al., 2004, Huang et al., 2005). These composites demonstrate huge changes in electrical conductivity σ with a small change of CNT concentration c (c<0.5 wt %) (Lisetski et al., 2007; Dierking et al., 2008; Lisetski et al., 2009; Zhao et al., 2009). Besides, the σ vs. c curve shows clear percolation behavior (Lebovka et al., 2008; Koval'chuk et al., 2008; Goncharuk et al., 2009). The huge conductivity increase may result in dielectric breakdown and local heating effects (Jayalakshmi & Prasad, 2009). Monitoring of electrical conductivity identified two time scales in reorientation dynamics of liquid crystal–nanotubes dispersions. These scales are associated with the reorientation of the liquid crystal texture (the short time scale) and with the reorientation of the carbon nanotubes (the long time scale) (Dierking et al., 2008). The electrical conductivity and the dielectric constant of LCs doped with carbon nanotubes demonstrate exctraordinary large changes in electric and magnetic field driven reorientation experiments (Dierking et al., 2004; Jayalakshmi & Prasad, 2009). In spite of these extensive studies, many aspects of LC-CNTs composites remained unclear. In particular, it was not well clarified the nature of electrical conductivity and charge transfer in different phase states of LC, at different concentrations of CNTs and in relations with the magnitude of applied voltage and frequency. The present paragraph is focused on these problems.

3.1 Dielectric spectra

Figure 1 presents typical dielectric spectra of 5CB-CNTs (a) and EBBA-CNTs (b) composites. The measurements were done at the temperatures falling within nematic phase of LC medium, T=297 K (5CB) and T=313 K (EBBA). The LC alignment is planar in case of 5CB and homeotropic in case of EBBA. According to Fig. 1, three frequency ranges, namely, f<10^2 Hz (A), 10^2 Hz<f<10^5 Hz (B) and f>10^5 Hz (C) can be distinguished. As is commonly accepted (Craig, 1995), the frequency range (A) reflects the near electrode barrier layers processes, the frequency range (B) corresponds to the bulk polarization and charge transfer and the frequency range (C) reflects the relaxation process caused by transition from the electronic and dipole polarization to only electronic polarization of LC phase.
In (A) and (C) ranges, the noticeable dispersions of the real ε' and imaginary ε'' components were observed. The data analysis has shown that Cole-Cole approximation (Haase & Wrobel, 2003; Chelidze et al., 1977) can be applied for estimation of corresponding low- and high-frequency times of dielectric relaxation, τ_A and τ_C:

$$\varepsilon^* = \varepsilon_\infty + (\varepsilon_o - \varepsilon_\infty)/(1 + i2\pi f\tau). \quad (2)$$

Here, ε^* is a complex dielectric permittivity, ε_o and ε_∞ are the limiting values for the frequencies f = 0 and f = ∞.
Fig. 1 demonstrates that CNT dopant substantially modifies dielectric spectra of LC. These changes in different frequency ranges are further analyzed.

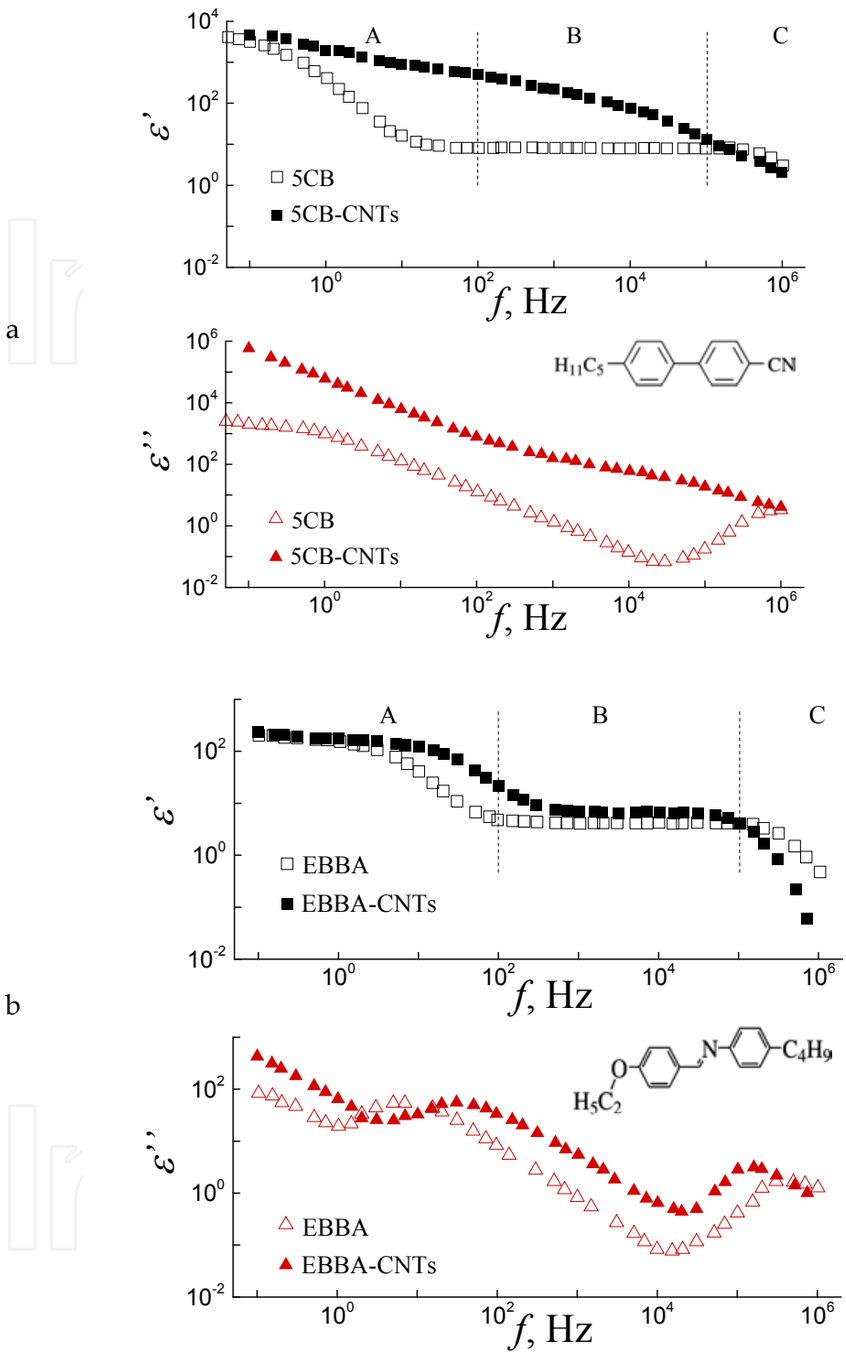

Fig. 1. Complex permittivity components ε' and ε'' versus frequency f for pure LC and LC-CNTs composites of 5CB (a) and EBBA (b). The concentration of CNTs c is 0.25 wt % (a) and 0.5 wt % (b). Chemical formulas of 5CB and EBBA are given on corresponding $\varepsilon''(f)$ graphs.

3.2 Electrical conductivity: Intermediate frequency range

We begin with the intermediate frequency range (B). In this range, large active resistances of the double electric layers (DEL) formed near the cell electrodes are shunted by their capacitance diminishing with a field frequency f (Koval'chuk, 1998; Koval'chuk, 2000; Barbero & Olivero, 2002; Koval'chuk, 2001b). Because of this, the range (B) characterizes volume properties of samples.

Based on formula (1), alternating current conductivity of the composite bulk can be estimated. In a general case, the alternating current conductivity σ of LC-CNTs samples can be represented as a sum of the frequency-independent ionic conductivity σ_i associated with LC, and the frequency-dependent electronic hopping conductivity σ_e, associated with CNTs, $\sigma=\sigma_i+\sigma_e$. These two contributions to the electric conductivity can be easily separated because of considerable frequency dependence of σ_e. The σ_e component becomes essential at CNT concentrations comparable and higher than a threshold concentration c_c corresponding to conductivity percolation discussed in the next subsection. The frequency-independent component σ_i is typical for ionic conductivity of liquids (Frenkel, 1955).

3.2.1 Percolation behavior

Different composites filled with CNTs typically demonstrate percolating behavior of the electrical conductivity σ, when sharp transition from the prevailing ionic to the prevailing charge hopping conductivity occurs at some threshold concentration c_c (Grossiord et al., 2006; Mamunya et al., 2008). At this concentration, the CNTs form a percolation network or cluster that spans the whole system (Stauffer & Aharony, 1992; Torquato, 2002). A theory predicts an inverse proportionality between c_c and the aspect ratio r of the conductive filler particles, $c_c \sim 1/r$ (Balberg et al., 1984; Foygel et al., 2005).

For CNTs with very high aspect ratio, typically, $r \approx 500\text{-}1000$, this theoretical estimation results in extremely low values of the percolation threshold, $c_c < 0.1$ wt %, which is in full correspondence with available experimental data (Lisunova et al., 2007; Mamunya et al., 2008; Lebovka et al., 2009).

The percolation behavior of electrical conductivity in different LC-CNTs composites was recently reported (Lisetski et al., 2007; Lebovka et al., 2008; Koval'chuk et al., 2008; Lisetski et al., 2009; Goncharuk et al., 2009). Fig. 2 demonstrates electrical conductivity σ versus filler concentration c curve for 5CB-CNTs samples, which is typical for the LC-CNTs composites. Here, the 5CB is planar oriented in a 16 μm cell. The measurements were carried out at 100 Hz, when frequency dependence of σ was practically absent and thus the ionic contribution to σ was dominating. The threshold increase of σ was observed for the values of CNT concentration c between 0.02 and 0.2 wt %. The experimental data were analyzed using the least-square fitting to scaling equation (Stauffer & Aharony, 1992)

$$\sigma \propto (c - c_c)^t . \tag{3}$$

As a result, the percolation threshold concentration c_c and conductivity transport exponent t were determined. The insert in Fig. 2 shows c_c and t versus temperature dependencies. There are evident the considerable temperature dependencies for both c_c and t.

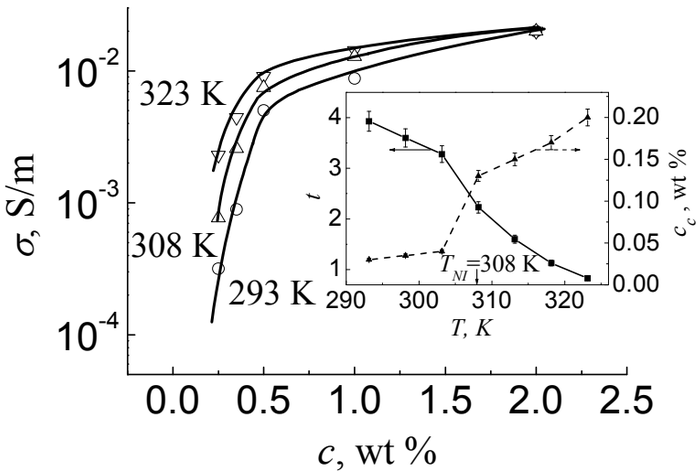

Fig. 2. Electrical conductivity σ versus concentration of nanotubes c in 5CB-CNTs composites for different temperatures T. Insert shows the conductivity exponent t and percolation threshold concentration c_c versus temperature T. The samples were planar oriented in a 16 μm cell, f=100 Hz.

Increase of the percolation threshold c_c with a temperature T is inessential within nematic mesophase ($T<T_{NI}\approx$308 K), however, it becomes noticeable in isotropic phase. At T=325 K the threshold concentration reaches $c_c\approx$0.2 wt %. Such character of $c_c(T)$ curve may be caused by number of effects such as change in the Brownian motion intensity, degree of the orientational order of nanotubes, etc. These factors influence degree of connectedness between the nanotubes and, as result, the percolation threshold (Kyrylyuk & van der Schoot, 2008). The effects of nanotubes' alignment on the percolation behavior were discussed recently, however, they still are not completely clear (Du et al., 2005; Behnam et al., 2007; Kyrylyuk & van der Schoot, 2008). More perfect alignment of CNTs inside the nematic phase is expected. However, it can be assumed that highly aligned nanotubes practically don't intersect each other and fail to create percolation paths. The highest electrical conductivity was experimentally observed for slightly aligned, rather than isotropic, composites (Du et al., 2005). Recent Monte Carlo simulations have also demonstrated that conductivity may be strongly dependent on the measurement direction and the degree of nanotube alignment (Behnam et al., 2007). Along with inducing alignment, nematic LC host stabilizes structure of CNTs damping their Brownian motions. Together with imperfect orientational order of CNTs it may explain the lower concentration threshold of CNTs in the nematic phase comparing with that in the isotropic state (see inset in Fig. 2).

Temperature decrease in the conductivity exponent t (see formula (3)), possibly, reflects changes in the conductivity mechanism and structure of the percolating clusters. The values of conductivity transport exponents $t\approx4/3$ and $t\approx2$ are characteristic for the ordinary 2d (two-dimensional) and 3d (three-dimensional) random percolations, respectively. Note that for the studied systems the 2d-3d crossover percolation behavior (Muller et al., 2003;

Lebovka et al., 2002) with $4/3<t<2$ was expected, because the restricted width of the cell (d≈16 μm) was comparable with the length of CNTs (l≈5-10 μm). Moreover, it was found that for the 3d composite filled with anisotropic particles t decreases substantially with increase in the aspect ratio (Foygel et al., 2005). The noticeable deviations from predictions of the standard percolation theory were also observed for systems with diverging local conductances, when distances between adjacent particles are broadly distributed (Johner et al., 2007). The reported transport exponent t often exceeds its classical values, reaching even the values as large as t=5–10 (Johner et al., 2008). Generally, the value of t extracted from the percolation data for CNT-filled composites may be dependent on the distribution function of distances between adjacent conducting particles (Mdarhri et al., 2008).
Note that $c_c(T)$ and $t(T)$ behave discontinuously in the vicinity of nematic-isotropic transition, T_{NI}≈308 K. It reflects strong dependence of the percolating characteristics on the phase state of LC host.

3.2.2 Temperature dependence and energy of activation

In the investigated range of temperature the electrical conductivity σ of the LC-CNTs composites increases with a temperature that is characteristic for the nonmetallic behavior. Moreover, temperature dependence of σ can be satisfactorily described by Arrhenius relationship (Lebovka, 2008):

$$\sigma \propto \exp(-W/kT), \tag{4}$$

where W is the activation energy, k is Boltzman's constant.
Figure 3 shows typical Arrhenius plots for 5CB-CNTs (a) and EBBA-CNTs (b) composites corresponding to different concentrations of nanotubes, c.

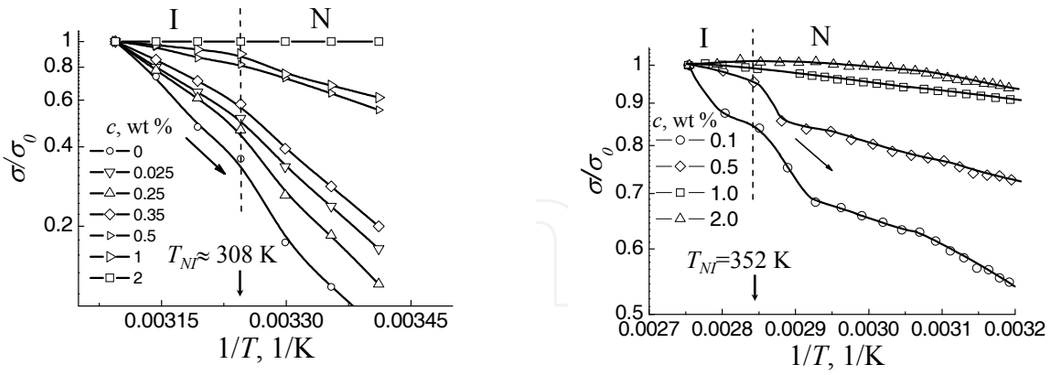

a b

Fig. 3. Relative conductivity σ/σ_0 versus inverse temperature $1/T$ for planar oriented 5CB-CNTs (a) and unoriented EBBA-CNTs (b) composites at different concentrations of nanotubes c. Here, σ_0 corresponds to the electrical conductivity at some reference temperature, which was 323 K in case (a) and 363 K in case (b). The cell gap d was 16 μm (a) and 500 μm (b), the frequency f was 100 Hz (a) and 1000 Hz (b). Arrows mark direction of temperature change.

In these experiments, the conductivity data were recorded in the cooling regimes accounting for the possible influence of the thermal pre-history. The obtained Arrhenius plots of $\sigma(T)$ curves were rather linear within the temperature ranges corresponding to nematic or isotropic phase; however, some deviations from linear behavior were observed near nematic-to-isotropic transition points. Moreover, the slopes were always larger in nematic phase than in isotropic phase; it corresponds to higher activation energy of the electrical conductivity in nematic phase. This can be explained by the restriction of the charge mobility in the nematic phase that is related to distortion of the LC director field in the vicinity of charge carriers (Belotskii et al., 1980). This distortion sphere surrounding the charged particle arises as a result of LC molecule orientation in the electric field generated by this particle.
Figure 4 presents examples of concentration dependencies of the activation energies determined from the Arrhenius plots in nematic phases of 5CB-CNTs and EBBA-CNTs composites.

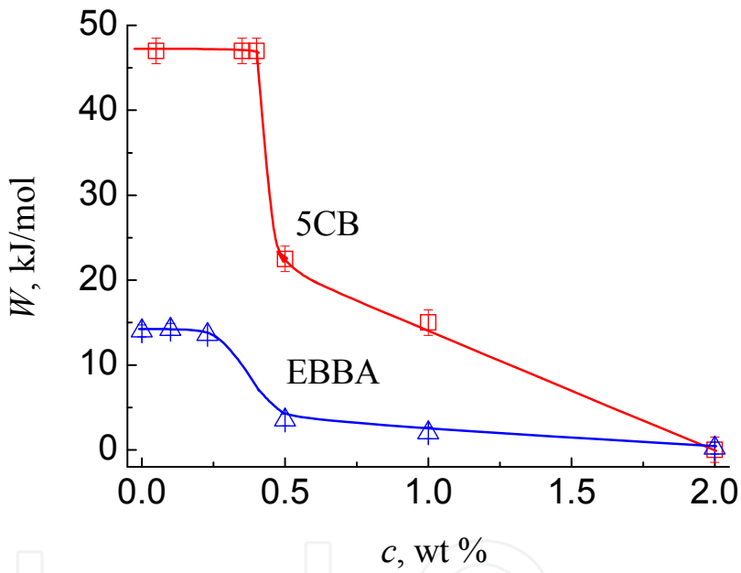

Fig. 4. Activation energy W of electrical conductivity versus concentration of CNTs c for planar oriented 5CB-CNTs and unoriented EBBA-CNTs composites. The values of W were determined from data corresponding to temperature ranges of nematic phases of 5CB and EBBA. The cell gap d was 16 μm (5CB) and 500 μm (EBBA), the frequency f was 100 Hz (5CB) and 1000 Hz (EBBA), the measuring voltage U was 0.25 V (5CB) and 1 V (EBBA).

Though values of W were determined for different LC media, for planar oriented (5CB) and unoriented (EBBA) composites, using different cell gaps and different protocols for σ measurements, similar tendencies were observed in $W(c)$ dependencies: W was constant at small concentrations below the percolation threshold and started to decrease above the percolation threshold approaching $W \approx 0$ kJ/mol at $c \geq 2$ wt %.

This behavior reflects the dominating role of ionic transport mechanism at concentrations below the percolation threshold with activation energy $W_i \approx 47$ kJ/mol (5CB) and $W_i \approx 15$ kJ/mol (EBBA). So, below the percolation threshold, the conducting LC-CNTs composites behave as semiconductors. This behavior is also typical for polymer-CNTs composites, where electrical conductivity is an increasing function of temperature, which was explained by thermally assisted hopping or charge tunneling between the conducting particles (Barrau et al., 2003). The decrease of W above the percolation threshold might be explained by the increasing role of charge transport through the CNT structure. Comparing with ionic conductivity of LC, electronic conductivity of CNTs is characterized by low temperature coefficient (Eletskii, 2009). This might decrease the apparent activation energy W of LC-CNTs composites and this tendency should essentially enhance with concentration of CNTs.

3.2.3 Hysteretic behavior and effect of positive temperature coefficient

It was previously demonstrated that temperature affects the spatial arrangement of CNTs in the LC matrix and changes percolation characteristics. The LC-CNTs composite typically displays also the electrical conductivity heating–cooling hysteresis and the pronounced effect of positive temperature coefficient of resistivity (PTC effect) (Lebovka et al., 2008; Goncharuk et al., 2009). Figure 5 presents examples of the electrical conductivity σ heating–cooling hysteresis for EBBA-CNTs unoriented composites in the thick cell ($d \approx 500$ μm). In these experiments, the composites that were initially solid were heated from room temperature up to 363 K and then cooled. The total time of the heating–cooling cycle was about 1 h. The hysteretic loops were most pronounced for CNT concentrations in the vicinity of the percolation transition ($c \approx 0.1$ wt %) and became inessential at higher values of c (figure 5).

The heating–cooling hysteretic behavior of electrical conductivity reflects strong agglomeration and rearrangement of nanotubes during the thermal curing. The abrupt decrease of the $\sigma(T)$ curve in the vicinity of melting point T_{SN} may be caused by several factors. Firstly, CNTs align within the nematic domains. It lowers degree of connectivity of the nanotubes. Besides, the initial network is also partially damaged by thermal expansion of the host EBBA matrix (Lebovka et al., 2008; Lebovka et al., 2009). At high concentration of CNTs the network formed in LC is rather strong because of high density of connectedness between the nanotubes. This strong network cannot be easily destroyed by the Brownian motion and LC reorientation intensified by heating and phase transitions. This explains weakening of hysteretic and PTC effects at $c > c_c$. Note that these effects are especially strong in thick cells, when the length of individual nanotubes, $l \approx 5$-10 μm, is small comparing with a cell gap d. In this case, the Brownian motion of individual nanotubes is unrestricted by nanoparticle interaction with the cell walls and so the Brownian motion and the LC orientational rearrangement are dominating factors in the observed reconstruction of CNTs network during thermal processing.

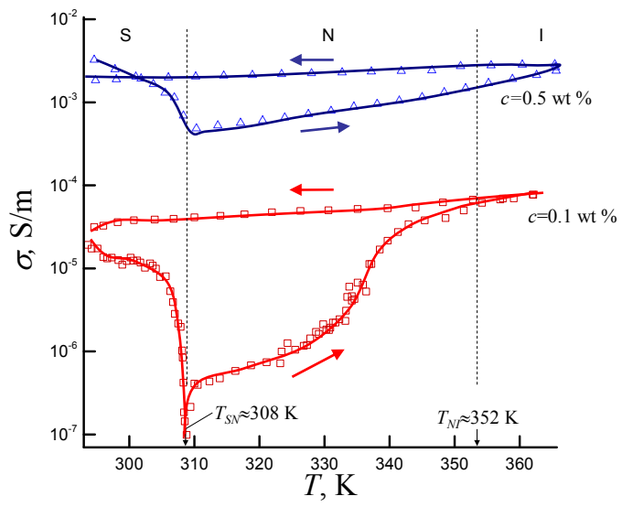

Fig. 5. Heating–cooling hysteresis of electrical conductivity σ for unoriented EBBA-CNTs composites. The measurements were made in a thick 500 μm cell, f=1 kHz, U=1V. The arrows show directions of temperature changes.

3.3 Frequency and voltage dependence

The frequency dependent contribution of electrical conductivity is common for disordered and/or highly alloyed solids (Gantmaher, 2005; Shklovskii & Efros, 1984). It was explained by correlated barrier hopping, tunneling or percolation model (Shklovskii & Efros, 1984; Mott & Davis, 1971, Pike, 1972). Typically, the power law dependences

$$\sigma \propto f^m \text{ or } \varepsilon'' \propto f^{m-1} \tag{5}$$

were observed. Here, m is a frequency exponent.

In the hopping transport model, the current carrier is assumed to hop over a potential barrier between neighboring localized sites and this model predicts that m is slightly lower than 1 and it decreases with rise of temperature. It is different from the tunneling model where the charge carrier is assumed to tunnel across the potential barrier. The tunneling model predicts smaller values of the frequency exponent ($0.4<m<0.8$) and temperature independent value of m. In the percolation theory, the critical exponent m is considered to be universal and determined only by statistical properties of the percolation clusters. The values of m obtained from numerical studies of random composites were in the range of 0.6–0.8 (Straley, 1977). The experimentally found m values near the percolation threshold were reported to be about 0.8–0.9 for carbon black composites (Jager et al., 2001), and 0.66 (Kim et al., 2003) or 0.85-0.9 (Liu et al., 2007) for carbon nanotube dispersions in polymers.

The studied dispersions of CNTs on the base of LCs demonstrated $\sigma(f)$ curves strongly depending on CNT concentration and temperature (Koval'chuk et al., 2008). The value of σ was practically independent on f at small concentrations of CNTs (c<0.1 wt % for 5CB) and became a power function of the frequency f at larger c. Examples of $\sigma(f)$ dependences for 5CB-CNTs composites are presented in the insert in Fig. 6a. It is evident that increase of CNT concentration c above c_c results in increase of both ionic σ_i and electronic σ_e contributions, while below $c_c \approx 0.1$ wt % the ionic contribution is dominating. The increase of

the ionic contribution σ_i with c can be partially caused by the increased concentration of ions introduced with impurities presented in CNTs. However, this factor is hardly a dominating one because of thorough purification of CNTs used in our studies. The more likely reason is facilitation of ionic transport through the charge exchange mechanism assisted by nanotubes. Such mechanism may be efficient due to the large dielectric constant of the CNTs, which results in strong attraction between impurity ions and nanotube surface (Jagota et al., 2005). This conclusion is supported by presence of double electric layer (DEL) shunting effect assisted by CNTs (see section 3.5). At CNTs concentrations between 0.1 and 0.35 wt %, σ_i =const and $\sigma_{e=}f^m$, which means that σ_i and σ_e can be easily separated. Above c=0.35 wt %, the component σ_e becomes frequency independent that complicates its separation. The frequency independence of σ_e may be the evidence of the transition from the hopping charge transfer to the quasimetallic electronic transfer typical for CNTs. This implies very tight network with direct connections between the nanotubes so that the conductivity barrier between them is rather low.

Figure 6a also presents frequency exponent m vs. the concentration c at 297K. The $m(c)$ dependence is a non-monotonic function with a maximum $m \approx 0.32$ near the concentration $c \approx 0.25$ wt %. Increase of m with c at c < 0.25 wt % reflects initial process of CNT cluster formation. In this interval of concentrations, the mechanism of electrical transport is mixed: electrical transport is governed by electron hopping/tunneling mechanism inside CNT clusters and by ionic mechanism between clusters. Above the percolation threshold, at high concentrations of CNTs (c>0.25 wt %), agglomeration of different clusters occurs and contacts between them are multiple. This results in formation of homogeneous ohmic conducting structure, when electron hopping/tunneling mechanism is inessential and electrical conductivity becomes frequency independent.

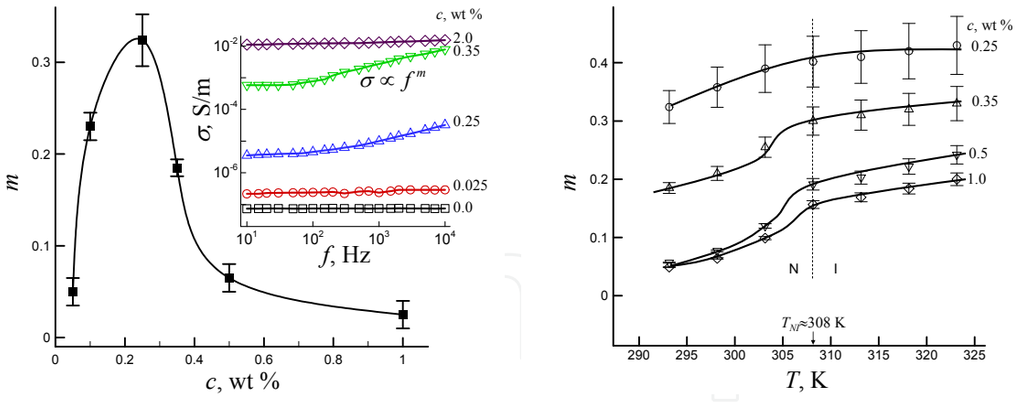

a b

Fig. 6. Frequency exponent m versus (a) CNT concentration (T=297 K) and (b) temperature for planar oriented 5CB-CNTs composites. Insert shows the conductivity σ versus frequency f plots for different concentrations of CNTs c.

The temperature dependencies of frequency exponents m for 5CB-CNTs composites are presented in Fig. 6b. The value of m is an increasing function of temperature. The evident changes in slope of $m(T)$ curves can be observed in the vicinity of nematic-isotropic

transition, T_{NI}≈308 K. The obtained data evidence a noticeable influence of the phase state of LC matrix on the charge transport mechanism. This effect can be easily explained accounting for the expected alignment of CNTs inside the nematic matrix (Dierking et al., 2004).

Note that observed behavior of the frequency exponent (rather small values of m (m<0.3) and positive thermal coefficient (dm/dT>0)) contradict with the classical hopping and tunnelling transport theories, predicting dm/dT<0 (Mott & Devis, 1971; Pike, 1972). The percolation theory also predicts rather high values of m, in the range of 0.6–0.8 (Straley, 1977). Note that critical exponent m may vary significantly depending on peculiarities of microstructure and morphology of the composite (Liu et al., 2007). However, at the moment, there is no theory available for explanation of the anomalously small values of m observed in 5CB-CNTs composites.

Large positive thermal coefficient dm/dT>0 obtained for nematic mesophase indicates enhancing of the frequency dependent contribution to electrical conductivity σ. This behavior, possibly, reflects the temperature changes in the percolating CNT networks inside the LC-CNTs composites. As was earlier discussed, temperature increase results in damage of the connectivity in percolation structures and, hence, in decrease of the "effective" filling concentration. Naturally, it resulted in increase of m with temperature T for concentrations above 0.25 wt % (Fig. 6b). This conclusion supports also the observed increase of the percolation threshold concentration c_c with temperature T (insert in Fig. 2).

A noticeably nonlinear behavior was also observed for current–voltage characteristics of LC-CNTs composites (Lebovka et al., 2008). Figure 7 presents voltage dependencies of electrical conductivity σ/σ_0 for EBBA-CNTs composites at different values of temperature T and concentration of nanotubes c.

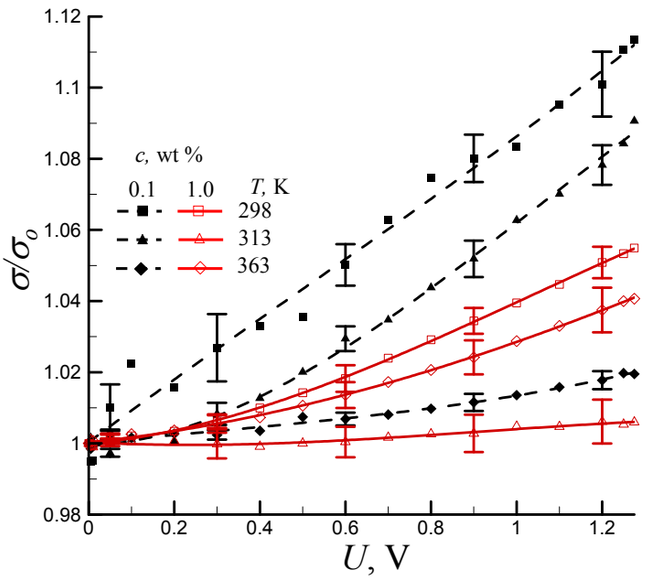

Fig. 7. Relative electrical conductivity σ/σ_0 versus measuring voltage U for composite EBBA-CNTs at different values of temperature T and concentration of nanotubes c. Here, σ_0 is electrical conductivity in the limit of U=0 V. The samples were randomly aligned in the 500 μm cells, f=1 kHz.

Such nonlinear behavior can be explained on the basis of hopping-tunneling model of transport disruption across the insulating LC regions between the CNTs, which predicts the following field dependence for electrical conductivity (Mott & Davis, 1971)

$$\sigma \propto \sinh(e\lambda_h E / kT), \tag{6}$$

where e is the elementary charge, λ_h is the average hopping distance, E is the applied electric field, and k is the Boltzmann constant.

The theory predicts weakening of the non-linear behavior with temperature T in full correspondence with experimental observations (Fig. 7). The most pronounced non-linear behavior was observed in the vicinity of the percolation threshold ($c_c \approx$0.05-0.1 wt %). It was becoming less explicit above the percolation threshold, where multiple direct contacts between different CNTs were formed. The observed weakening of the current–voltage nonlinear behavior above the percolation threshold (Fig. 7) correlates with decrease of electrical conductivity activation energy (Fig. 4).

3.4 Dielectric relaxation and near-electrode processes: Low frequency range (A)

The dielectric spectra in the most low frequency range (A) (f<10^2 Hz) are mainly determined by the near-electrode processes and electron exchange between electrodes and ions (Koval'chuk, 1998; Koval'chuk, 2000; Barbero & Olivero, 2002; Koval'chuk, 2001c). In this range, the most important changes, provoked by presence of CNTs, were observed for the imaginary (ac conductance) component ε'', while changes for real (capacitive) component ε' were smaller. At low frequencies (f<0.5 Hz), increase of the component ε'' was observed by doping LC (both 5CB and EBBA) with CNTs (Fig. 1).

This behavior can be explained by enhancement of the electron component in electrical transport through the near-electrode layers, governed by the presence of CNTs in a composite. In fact, the CNTs serve as shunts of the double electrical layers providing paths for the electron exchange between electrodes and impurity ions inside LC.

The shunting effect observed at low frequencies (f<0.5 Hz) and related with the presence of CNTs was characterized in terms of the dielectric loss tangent, tan δ_s, which is given by

$$\tan\delta_s = \varepsilon'' / \varepsilon'. \tag{7}$$

Note that tan δ_s characterizes dielectric loses in the near electrod layers and thus is a surface parameter.

Figure 8 presents tan δ_s as a function of CNT concentration c for 5CB-CNTs composites.

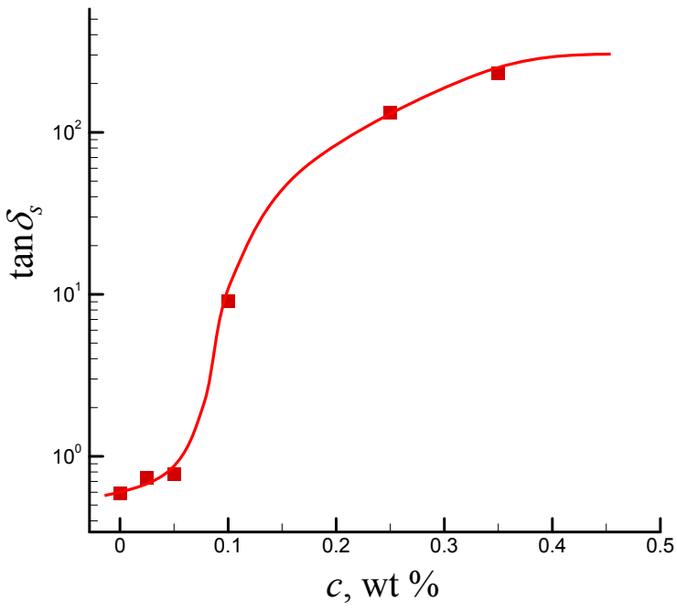

Fig. 8. Dielectric loss tangent tan δ_s versus CNTs concentration c for planar oriented 5CB-CNTs composites in a 16 μm cell at T=293 K, f=0.1 Hz.

At small concentrations of CNTs (c<0.05 wt %), tan δ_s is rather small and dielectric parameters of the near-electrode layers are determined by the properties of 5CB itself. However, the abrupt rise of tan δ_s in the interval of c values between 0.05 and 0.1 wt % evidences about formation of effective shunting paths as elements of a percolation network of CNTs characterized by the same concentration threshold.

The width of the near-electrode layers λ_s can be estimated (Koval'chuk, 2001a; Koval'chuk, 2001c):

$$\lambda_s \approx d\varepsilon_o^C / 2\varepsilon_o^A, \tag{8}$$

where ε_o^A and ε_o^C are the limiting values of ε for the frequency ranges (A) and (C). For example, for pure EBBA, the estimated width of near-electrode layer λ_s is about 0.3 μm and it is practically independent from the cell thickness d (Fig. 9). The doping of EBBA by CNTs (0.5 wt %) results in a noticeable increase of λ_s. This might be caused by increased concentration of ionic impurities or structural modification of DELs in presence of CNTs.

The low-frequency relaxation process characterized by the time τ_A we assign to dipolar polarization relaxation of LC molecules. These molecules can be anchored to the surfaces of the cell and to a skeleton of CNTs acting as a spatially distributed surface in LC host. For pure EBBA, τ_A is an increasing linear function of a cell gap d. The linear increase of the dipole relaxation time with d in the near-electrode zone τ_A was also observed for the planar oriented LC media (Yaroshchuk et al., 2005). It was established that value of τ_A decreases with the increase of electric conductivity. The similar tendency observed for EBBA doped with CNTs (Fig. 9) may be explained by high shunting efficiency of CNTs in the near-electrode zones and the ionic impurities introduced in LC together with CNTs.

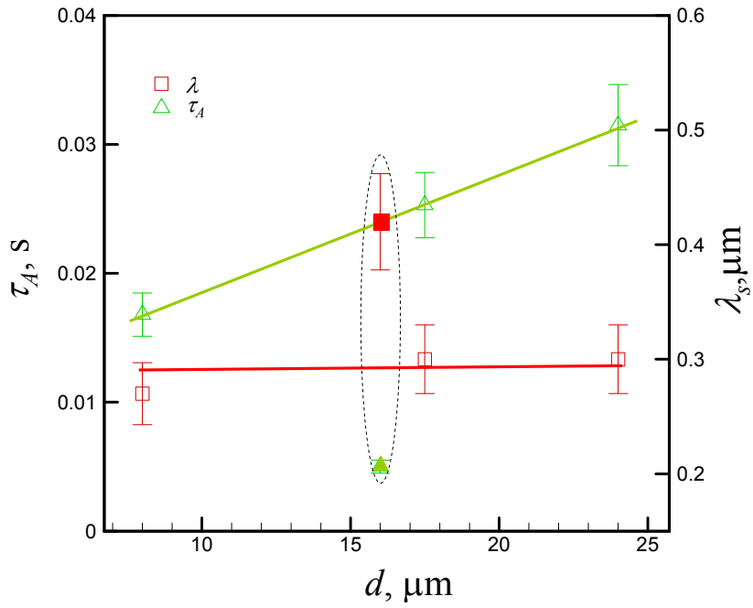

Fig. 9. Near-electrode layer width λ_s and low-frequency relaxation time τ_A vs. a cell gap d for pure EBBA (open symbols) and EBBA-CNTs composite (c=0.5 wt %) (filled symbols). The EBBA media was homeotropically oriented.

3.5 High frequency dielectric relaxation: High frequency range C

The high frequency dielectric relaxation time τ_C was practically independent of d for pure EBBA (τ_C≈0.67 μs), and doping by CNTs (0.5 wt %) resulted in increase of τ_C (τ_C≈2.5 μs). The similar tendency of τ_C to increase was observed also for 5CB-based composites, where τ_C≈0.56 μs for pure 5CB and τ_C≈0.94 μs for 5CB-CNTs (0.5 wt %) composite.

4. Electro-optic studies of LC-CNTs composites

Electrically controlled birefringence is a major property of LCs utilized in liquid crystal displays (LCDs), optical shutters, LC lenses and other LC devices. The present section considers influence of CNTs on the electro-optic properties of LC layers. It consists of three subsections. Subsection 4.1 refers to recent improvements of reversible LC response achieved owing to CNT addition. Subsection 4.2 is based on our original results concerning the irreversible electro-optical response of the LC-CNTs systems named as electro-optic memory (Dolgov et al., 2008; Dolgov et al., 2008a). At last, subsection 4.3 describes enhancement of the memory effect in the systems with induced chirality (Yaroshchuk et al., 2010).

4.1 Reversible electro-optic response

Generally, nematic LC devices utilize reversible response of LC layers on the applied voltage (Blinov & Chigrinov, 1996). The characteristics of this response, such as controlling voltage, switching on and off times, contrast ratio, etc., are quite important operational parameters of the LC devices. The major trend in improvement of these parameters is associated with synthesis of new mesogenic compounds and development of new eutectic

LC mixtures on their base. The other direction recently arose due to intensive development of nanotechnologies. Some types of nanoparticles turned out to be very useful fillers fundamentally expanding the range of mechanical, dielectric, magnetic, and optical characteristics of LCs (Qi & Hegmann, 2008).

Among nanoparticles as fillers for LCs, carbon nanotubes take special place. Due to strong shape anisotropy they possess strong anisotropy of polarizability. Therefore embedding even small amount of CNTs (c<0.05 wt %) into liquid crystal host may essentially increase (case of LC with $\Delta\varepsilon>0$) (Lee et al., 2004) or decrease (case of LC with $\Delta\varepsilon<0$) (Huang et al., 2005) dielectric anisotropy. Driving voltage is inversely proportional to the module of $(\Delta\varepsilon)^{1/2}$ and so it may be essentially influenced by carbon nanotubes.

As it was mentioned in section 3.2.1, carbon nanotubes (at $c\geq$0.01 wt %) generally enhance conductivity of LCs. However, at minute amount of nanotubes (~0.001 wt %), this effect is inessential. At the same time, the nanotubes may affect significantly the number of free-moving ions and their distribution within the cell by means of ion adsorption and shunting of double electric layers (see section 3). As a result, a minute doping by carbon nanotubes allows to suppress a number of parasitic ionic effects peculiar to LC electro-optic devices, such as a field screening (Lee et al., 2004), image sticking (Baik et al., 2005), transient current (Chen & Lee, 2006), back flow (Huang et al., 2005; Chen et al., 2007) and hysteresises of capacitance and transmittance (Lee et al., 2004; Baik et al., 2005). This results in lowering of driving voltage (Lee et al., 2004) and shortening of response times (Chen et al., 2007). Along with nematic LCs, CNT dopant may improve properties of LCDs based on ferroelectric LCs. Specifically, it fastens response of the deformed helix ferroelectric liquid crystal displays (Prakash et al., 2009). The changes in structure and resistivity of double electric layers and the composite's rotational viscosity due to carbon nanotubes are discussed as the possible reasons of such speeding-up of the electro-optic response.

4.2 Irreversible electro-optic response: effect of electro-optical memory

The irreverible response is not typical for nematic LCs commonly used in LC devices. However, the embedded nanoparticles grant this property to LCs (Kreuzer et al., 1992; Glushchenko et al., 1997). Regarding LCs filled with CNTs, interesting memory effect has been recently observed in isotropic phase of LC material (Basu & Iannacchione, 2008). It consists in irreversible change of dielectric constant of LC-CNTs composite under the applied voltage and is explained by formation of pseudonematic domains near the CNTs reorienting in the electric field. Since there is no restoring force in the isotropic phase, after the field is off, these domains keep the orientation induced in the electric field.

In what follows, a different memory effect is considered. It is peculiar only to the nematic mesophase of LCs with $\Delta\varepsilon<0$ homeotropically aligned before the action of the electric field. Besides, to realize this effect, the concentration of CNTs in the LCs should be considerably higher (c>0.01 wt %) then in the case of composites with the reversible electro-optic response (c~0.005 wt %).

To elucidate this memory effect, let us consider transmittance η of the samples placed between pair of crossed polarizers as a function of the applied voltage U. The $\eta(U)$ curves for the EBBA-CNTs samples are presented in Fig. 10.

In these experiments the voltage was smoothly increased to 60 V and then decreased to 0 V. One can notice that the $\eta(U)$ curves have oscillating character. The $\eta(U)$ oscillations mean that optical phase incursion during the switching of LC is much more higher than $\pi/2$. The

saturation of this curve implies that, together with the bulk, the surface fraction of LC is reoriented in the field. It is evident that the neat LC demonstrates reversible electro-optic response (Fig. 10a). A small hysteresis (1–2 V) can be explained by screening of the applied field with the DELs formed near the cell electrodes (Baik et al., 2005). A very similar character of $\eta(U)$ curves is observed for the LC-CNTs composites with a small content of CNTs (c<0.01 wt %).

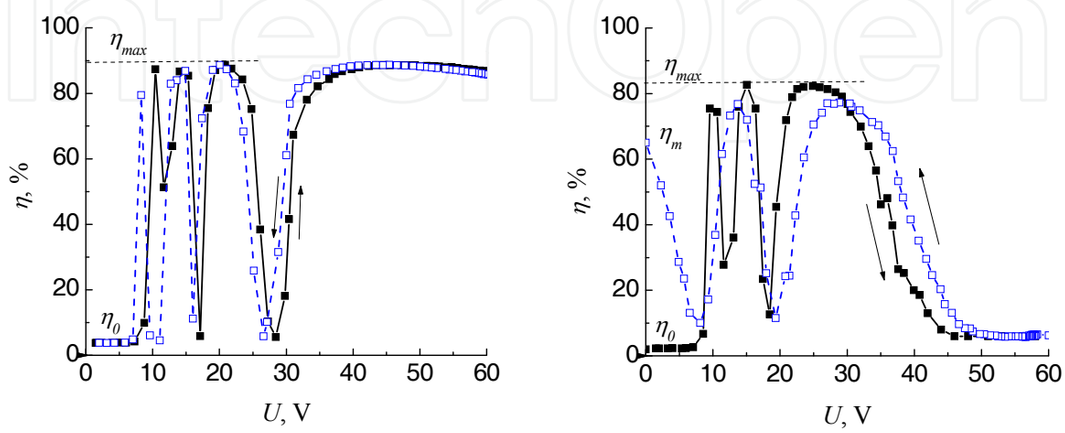

a b

Fig. 10. Dependences of light transmittance η on applied voltage U for EBBA doped with different concentrations of CNTs: a) 0 wt %; b) 0.05 wt %. Arrows indicate the increase and drop of voltage.

The situation, however, changes with a further increase of c. In this case, the oscillations are less pronounced for the reverse part of $\eta(U)$ curve. In addition, transmittance of the sample after the voltage decrease to zero, η_m, is sufficiently higher than the initial transmittance η_0 (Fig. 10b). This means that, to some extent, the cell memorizes transmittance realized in the electric field. This effect named as the effect of electro-optical memory can be characterized by the memory efficiency parameter M (Dolgov et al., 2008; Dolgov et al., 2009):

$$M=(\eta_m-\eta_0)/(\eta_{max}-\eta_0)*100\ \%, \quad (9)$$

where η_{max} is the maximal value of light transmittance (Fig. 10).
For the EBBA-CNTs composites under consideration, dependence of the memory parameter M on concentration of CNTs c is nonmonotonic. The $M(c)$ curve rapidly grows, reaches maximum at nanotube concentrations 0.02-0.05 wt % and then gradually decreases (Fig. 11, curve 1).
The initial rapid growth of this curve has percolation origin, which will be discussed below. The decay is apparently connected with a decrease in the effective voltage applied to the composite layer due to a marked increase in conductivity of the sample at high concentrations of carbon nanotubes.

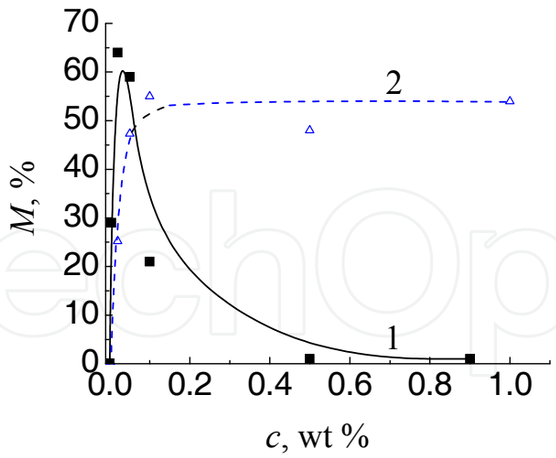

Fig. 11. Memory efficiency M as a function of the weight concentration of nanotubes c for the mixtures based on different liquid crystals: (1) EBBA-based series; (2) MLC6608-based series. The curves (1) and (2) are measured at temperatures 313 K and 297 K, respectively.

Generally, the memory efficiency M grows and reaches saturation with voltage application time τ. The memory reaches the state of saturation slower at lower driving voltages. For instance, at U=50 V the saturation time is 60 s, while at U=20 V it is 270 s. No electro-optical memory is observed at voltages U<10 V.
The effect of electro-optical memory is so pronounced that can be easily seen with a naked eye by sample observation through crossed polarizers (Fig. 12).

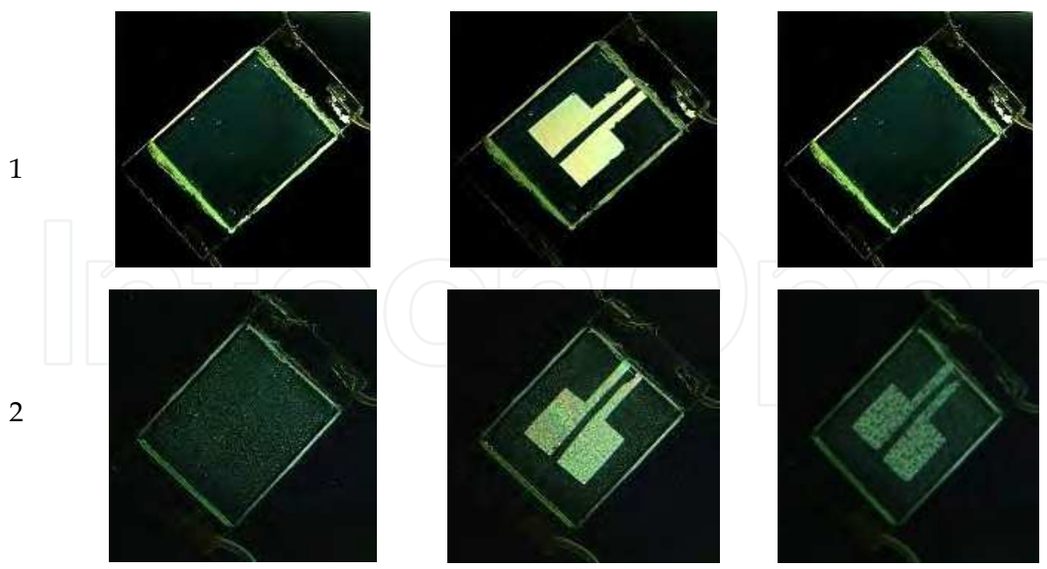

Fig. 12. Photographs of cells placed between the crossed polarizers and filled with neat EBBA (row 1) and EBBA doped with 0.02 wt % (row 2) of carbon nanotubes: a) initial off-state; b) U=60 V, f=2 kHz; c) off-state after field application. Voltage was applied to the central rectangular area of the sample.

One can see that neat LC cell switches homogeneously from the initial homeotropic to the planar state under the applied voltage. After the voltage switch-off LC returns to the initial state with homeotropic alignment. Similar behaviour is observed for the LC with minute (<0.01 wt %) concentrations of CNTs. LC suspensions with higher amount (c>0.01 wt %) of CNTs switch in the field to the random planar state. This state remains after switching off the voltage and causes high residual transmittance of the sample, i. e. electro-optical memory. Note that the memory can be completely or partially erased by applying to the sample mechanical stress, low frequency voltage (f = 10–50 Hz, U > 30 V) or by the transition of a system to crystalline or isotropic states with subsequent return to the mesophase.

It was further found that, besides EBBA, the described memory is peculiar to MLC6608 and MLC6609, LC mixtures with $\Delta\varepsilon$<0 and nematic mesophase at room temperatures. So there is no need in keeping samples at elevated temperatures during electro-optic tests. It simplifies measuring process in comparison with the EBBA-based mixtures. Below we present results for the MLC6608-based suspensions, but the results for the MLC6609-based samples are quite similar.

The $\eta(U)$ curves for the neat MLC6608 and MLC6608-based suspension are presented in Fig. 13. It is evident that these curves have smaller number of pulsations than the corresponding curves for EBBA-CNTs samples. This is caused by a smaller value of birefringence of MLC6608 (Δn=0.083 vs. Δn=0.25 for EBBA, Table 1).

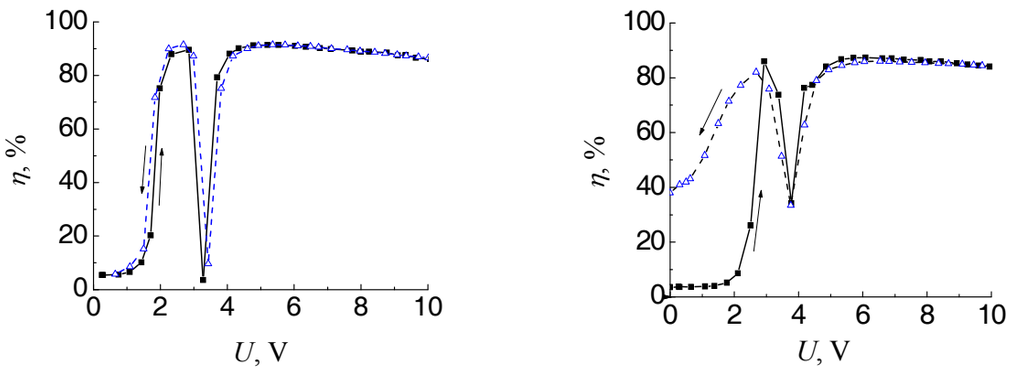

Fig. 13. Transmittance η vs. the voltage U curves for the MLC6608-CNTs composites with different concentrations of nanotubes: (a) 0 wt %; (b) 0.05 wt %. Arrows mark the plots obtained for the increasing and decreasing voltages.

The absolute value of dielectric anisotropy is much higher for MLC6608 than for EBBA (-4.2 vs. -0.13, Table 1). This results in much smaller values of saturation voltages for MLC6608-based mixtures (4–5 V) comparing with those for EBBA-based samples (35–40 V).

The maximal memory efficiency for MLC6608-based suspensions is similar to that for the EBBA-based samples (M=55-60 %). At the same time, the concentration dependences of M are essentially different. While the $M(c)$ curve for EBBA-CNTs series goes through the maximum (Fig. 11, curve 1), the corresponding curve for MLC6608-CNTs series rapidly grows and saturates at c~0.1 wt % (Fig. 11, curve 2). As discussed later, this is caused by different concentrations of ionic impurities and different structuring of CNTs in these LCs.

According to Fig. 14b, the appearance of the cells filled with MLC6608-CNTs composites is similar to that of analogous EBBA-based samples (Fig. 12); they contain areas with uniform homeotropic alignment not subjected to electric field and areas with the random planar alignment realized after the field cycle application. The memorized alignment state typically consists of islets of LC in a random planar state surrounded by the aggregates of CNTs.
It is important to note that for the suspensions based on LCs with $\Delta\varepsilon>0$, particularly for the 5CB, the memory effect is absent. The dependence of memory on a sign of dielectric anisotropy of LC will be elucidated in subsection 5.3.

4.3 Enhancement of memory effect by chiral dopant

The electro-optic memory effect described above is of considerable interest for applications. It suggests new principle for information displaying and storage in the LC based systems and thus can be designed for application in erasable memory cells, bistable displays, etc. These applications require essential improvements of the operational characteristics of LC-CNTs composites, first of all memory efficiency, erasure and recording times.

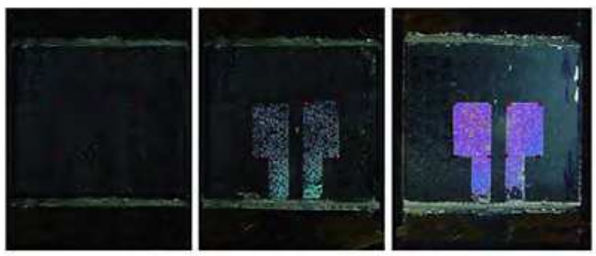

Fig. 14. The cells filled with LC MLC6608 (a), MLC6608-CNTs (c=0.02 wt %) (b) and MLC6608-ChD-CNTs (c=0.02 wt %, c_{ch}=0.1 wt %) (c) composites viewed between a pare of crossed polarizers. A cycle of electric field (30 V, 1 min) was applied to rectangular areas in the middle of the cells.

This paragraph describes the method of essential improvement of the memory efficiency M. The improvement is achieved by inducing chirality in LC host. This chirality causes additional force stabilizing the state of planar alignment realized in the electric field. Using this principle, efficiency of electro-optic memory can be practically doubled.
In our experiments the chirality of LC MLC6608 was induced by doping it with a small amount of chiral dopant (ChD) S811 from Merck. These studies were carried out in two stages. First stage was aimed at an optimization of chiral dopant concentration, c_{ch}. The increase of c_{ch} strengthens twisting tensions in the MLC6608. It was revealed that at $c_{ch}\leq$0.1 wt % anchoring forces satisfactorily balance these twisting tensions thus stabilizing homeotropic alignment. At $c_{ch}\geq$0.15 wt %, the anchoring forces can not restrain the twisting forces anymore that leads to a formation of various helical structures; at c_{ch}=0.15 wt % the filamentary texture is formed, which transforms in the fingerprint texture at higher concentrations. The concentration c_{ch}=0.1 wt % was selected for further preparation of LC-ChD-CNTs samples. It was the maximal value at which a uniform homeotropic alignment was preserved.
The $\eta(U)$ characteristics for the LC-ChD-CNTs sample, as well as for the reference LC-ChD sample are given in Fig. 15.

As is evident, the LC-ChD sample demonstrates reversible response. In turn, transmittance of LC-ChD-CNTs sample changes irreversibly showing high residual value in a zero field. The memory parameter estimated according to (9) is M=82 %. The corresponding value estimated for the LC-CNTs counterpart with the $\eta(U)$ curve presented in Fig. 13b is 0.44. This means that chiral dopant increases memory efficiency almost by factor 2. The strengthening of the memory effect in the samples containing chiral dopant can be seen even by naked eye (Fig. 14). The observation in polarizing microscope demonstrates that the planar state has an islet structure in the LC-CNTs samples, and a continuous structure in the LC-ChD-CNTs samples. This explains the increased memory efficiency of LC-ChD-CNTs samples.
The enhanced affinity of LC-ChD-CNTs samples to planar alignment might be explained by the enhancement of forces resulting in planar alignment. In the LC-ChD-CNTs samples, the force associated with a CNT network is magnified by a twisting force, which eventually destroys homeotropic alignment.

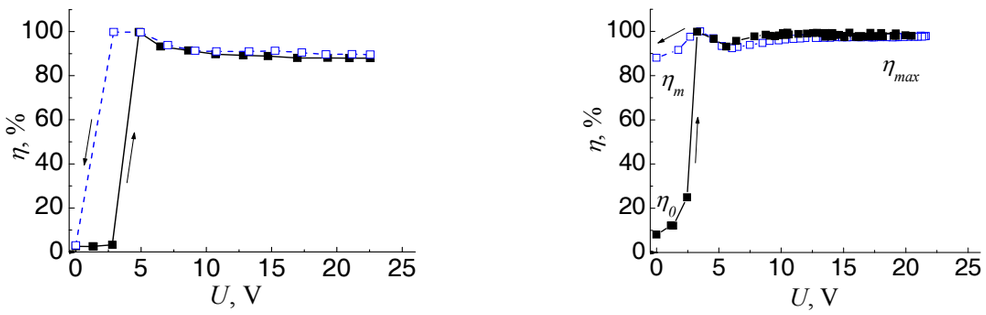

a b

Fig. 15. The transmittance η vs. applied voltage U curves for the cells filled with MLC6608-ChD (c_{ch}=0.1 wt %) (a) and MLC6608-ChD-CNTs (c=0.02 wt %, c_{ch}=0.1 wt %) (b) compositions. The arrows point directions of voltage ramping up and down.

It worth mentioning that, in spite of the memory enhancement of LC-CNTs samples, the twisting force by itself does not cause a memory effect (the case of LC-ChD samples, Fig. 15a). This suggests that the described memory effect is an intrinsic feature of samples containing CNTs.

5. Structural peculiarities of LC-CNT composites and structural transformation under the applied field

This paragraph consists of three subsections. Subsection 5.1 is introductory. It briefly refers to structuring of CNTs in LC hosts and methods of stabilization of CNTs in the LCs. In addition, several known effects connected with the influence of electric field on the CNT aggregates are reviewed. Subsection 5.2 is based on original results and considers microstructuring of the memory type LC-CNTs composites. Particularly it is shown how the electrohydrodynamic flows developed in LC host change the structure of CNTs and promote formation of the memory state. Finally, in subsection 5.3, physical model of electro-optic memory is suggested based on the microstructural observations and results of electro-optical and dielectric measurements.

5.1 Structural transformations in LC-CNTs composites without electrohydrodynamic flows

CNTs strongly attract with each other by van der Waals forces. Therefore they form more or less developed system of aggregates in a liquid host. Weak aggregation of CNTs is observed in the polar aprotic solvents like dimethylformamide (Liu et al., 1999), *N*-methyl-2-pyrrolidone (Giordani et al., 2006), the chlorinated hydrocarbon dichloroethane (Baik et al., 2005), and the polar protic compound ethyl alcohol (Huang & Pan, 2006).

In LC matrices the nanotubes aggregate quite intensively. This is a challenge for the majority of applications demanding LC-CNTs composites with high and uniform dispersion of CNTs. To achieve this, several methods are proposed.

In one of these methods strong aggregation of CNTs was prevented by their initial dispersion in organic solvents with next addition of LC (Baik et al., 2005). After evaporation of solvent one can obtain CNTs dispersed in LC medium. However, one of the drawbacks of this dispersion technique is the undesired residual solvent effect, which may influence quality of LC phase.

Another method lies in modification of CNT surface for enhanced compatibility with LCs. In this case CNTs bear on their surface small molecules, polymers or inorganic species (Trushkevych et al., 2008). But such modification can affect intrinsic mechanical, electrical and optical properties of CNTs (Bahr et al., 2001).

The more simple technique is just ultrasonication of CNTs in LCs without special dispersing agents. Centrifugation and decantation separate the suspension from big aggregates and may be used as additional methods after ultrasonication of CNTs (Chen et al., 2007).

Influence of electric field on CNT aggregates dispersed in LCs turned out to be quite manifold. The electric field may influence structure of CNTs directly or indirectly. One of examples of direct action is a drift of individual CNTs in LC under strong electric fields due to electrophoretic forces (Baik et al., 2006; Chen et al., 2008a). Movement of CNTs in the uniformly aligned LC may be traced due to specific light scattering appearing from the moving nanotube. It was also revealed that the internal forces appearing due to polarization of nanotubes in the electric field may cause structural changes of CNT aggregates. For example, the in-plane electric field of 5.67 V/μm at 60 Hz causes reversible four times elongation of CNT aggregates in the superfluorinated nematic LC (Jeong et al., 2007).

A striking example of the indirect action is the control of CNTs alignment by LC reorientation in electric field (Dierking et al., 2004; Dierking et al., 2008). As a rule, this mechanism does not involve essential LC flows. At the same time, at certain experimental conditions, the electrohydrodynamic (EHD) flows are highly intensive in LC cells (Blinov & Chigrinov, 1996). They can also be realized in the LCs doped by CNTs (Chen et al., 2008b). The next section elucidates structural reconstruction of CNT aggregates under the EHD flows resulting in effect of electro-optic memory. It is based on our recent results published in (Dolgov et al., 2008; Dolgov et al., 2009).

5.2 Structural transformations in the LC-CNT composites with electrohydrodynamic flows

Similarly to other LC-CNTs composites (Dierking et al., 2004; Jeong et al., 2007; Lee et al., 2004; Baik et al., 2005), the memory type EBBA-CNTs composites contain CNTs in aggregated state. Big aggregates are clearly visible in a polarizing microscope. The size of aggregates increases up to tens and even hundreds of microns with increase in the CNT

concentration. The single aggregates observed at c<0.02 wt % are assembled into a continuous network, when c>0.1 wt %.

The evolution of the samples structure under the action of the high frequency electric field (f=2 kHz) depends essentially on the concentration of nanotubes. In the neat EBBA and EBBA doped with a very small amount of CNTs (c<0.002 wt %), the initial homeotropic alignment state (Fig. 16a) switches to the uniform planar state (Fig. 16b) at voltages ~10 V. At higher voltages, the classical electrohydrodynamic instabilities develop in these samples. Laminar flows, revealing itself in the form of the Kapustin-Williams domains, arise at U=80 V (Fig. 16c) (Blinov & Chigrinov, 1996). As the voltage increases, the flow patterns become complicated and transform to turbulence patterns at voltages 110–120V (Fig. 16d). The EBBA samples return to the initial homeotropic state after switching off the field (Fig. 16a). In the samples with higher concentrations of nanotubes (c~0.02–0.05 wt %), the development of EHD instabilities is different. At U~10 V, LC switches from the homeotropic to the planar state (Figs. 17a, b). As the voltage increases, EHD flows appear near the aggregates of CNTs. The further increase in the voltage leads to the broadening of flow areas (Fig. 17c), which overlap (at U~40 V) and finally occupy the whole volume of the sample. In this process, the Kapustin-Williams domains appear in some areas of the sample.

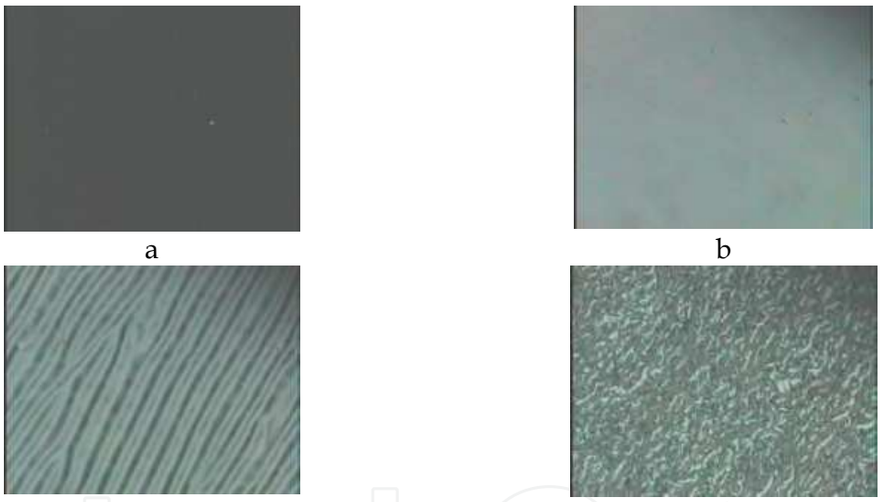

Fig. 16. Microphotographs of the EBBA layer subjected to alternating voltage (f=2 kHz): (a) initial state (U=0 V); (b) U=10 V; (c) U=80 V; (d) U=120 V. The sample is viewed between a pair of crossed polarizers. The photographs show development of electrohydrodynamic flows in the layer of pure EBBA.

However, regular structure of these domains was not observed. It is evident from Figure 17 that the turbulence results in the grinding of aggregates and the effective dispersion of CNTs.

Note that in samples with higher concentration of nanotubes (c>0.1 wt %) hydrodynamic motions arose too, but they did not influence essentially the morphology of aggregates. This is caused by lowering of the actual voltage and sample heating due to the essentially increased conductivity (Shah et al, 2008).

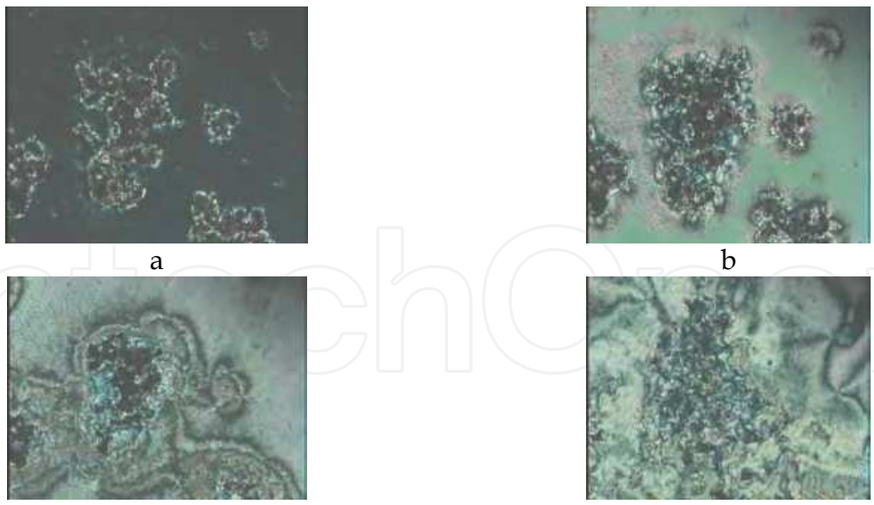

Fig. 17. Microphotographs of the layer of EBBA-CNTs composite (c=0.05 wt %) subjected to alternating voltage (f=2 kHz): (a) initial state (U=0 V); (b) U=10 V; (c) U=20 V; (d) after removing the field (U=0 V). The sample is viewed between a pair of crossed polarizers. The photographs show development of electrohydrodynamic flows in the layer of EBBA-CNTs composite.

The grinding of CNT aggregates and their motion in the EHD flows differs from the earlier described effects of the CNT structure reorganization related to the electrostatic and electrophoretic forces (Jeong et al., 2007; Baik et al., 2006). The dispersion process described above was observed only in the LCs with pronounced EHD instabilities.

In contrast to samples with c<0.002 wt %, the samples with 0.02<c<0.5 wt % remain in the random planar state and have the schlieren microscopic texture after the field switch-off (Fig. 17d). This texture caused the residual transmittance T_m and thus the memory effect.

Comparing with EBBA-based samples development of EHD instabilities in MLC6608 based samples has some differences. In contrast to EBBA, MLC6608 does not reveal any hydrodynamic flows up to 100 V. This is caused by the fact that the ionic conductivity of MLC6608 is one order of magnitude less than that of EBBA. It is well known (Blinov & Chigrinov, 1996), that the sufficient amount of ionic impurities in LC is needed for the development of hydrodynamic instabilities.

The EHD flows in MLC6608 appear only after addition of carbon nanotubes. As in EBBA-based composites, two steps of the LC response to the applied field can be selected: at first, at U=4–9 V, the Friedericksz transition occurs, and then, at higher voltages, hydrodynamic flows develop. In contrast to EBBA-based composites, hydrodynamics in MLC6608-based samples occurs in the form of turbulent flows without the stage of Kapustin-Williams domains. These flows begin to develop just after the Friedericksz transition in the vicinity of CNT aggregates. The areas of turbulence grow with the applied voltage and occupy the whole volume of the sample at 20–40 V. The developed flows result in the grinding of the aggregates of nanotubes. This effect can be considered as a practical method for in situ dispergation of CNTs in a LC medium.

5.3 Percolation structures of CNTs and mechanism of electro-optic memory

According to results of dielectric studies (section 3), the conductivity of LC-CNTs composites demonstrates pronounced percolation behavior. A steep increase of conductivity with concentration of CNTs is caused by self organization of these conductive particles resulting in formation of continuous spatial network percolating through the LC layer.

The results of structural studies of LC-CNTs composites with EHD instabilities (subsection 5.2) lead us to conclusion that the networks of CNTs formed before and after the application of an electric field are different. Before switching on the field, CNTs agglomerate in big clusters forming a network structure at high concentrations (c>0.5 wt %). A much finer structure occurs after the application of an electric field. The massive aggregates of nanotubes crushed in the EHD flows are assumed to form a fine network stabilizing the planar state of LC. This is confirmed by the two-order increase of sample conductivity after development of EHD instabilities.

The decisive role of hydrodynamic flows in the formation of the fine CNT network and thus the memory is confirmed by other experiments. First, the memory effect was not obtained in the composites based on LC 5CB ($\Delta\varepsilon$>0), in which EHD effects are not realized. Second, the memory effect was not observed neither in EBBA- nor in MLC6608-and MLC6609- based composites reoriented from the homeotropic to the planar state by the magnetic field. It is well known that a magnetic field causes no hydrodynamic flows in LC.

The formation of fine CNT network is closely related to memory effect. As was clarified above, the electro-optic memory is caused by the metastable planar LC alignment formed after the field is off. This alignment is stabilized by the network of CNTs acting as a spatially distributed alignment surface for LC. The alignment force of this network overcomes corresponding force of the aligning substrates restricting suspension layer. The analogous mechanism was earlier considered for LC-aerosil composites (Kreuzer et al., 1992; Glushchenko et al., 1997). It is known that such a system is characterized by the pronounced electro-optical memory effect caused by orientational LC transition from the spatially random to oriented state. The oriented state was metastable in a zero field because it was maintained by the network of aerosil particles.

To resist elastic tensions and so maintain planar alignment of LC phase in the LC-CNTs composites, the CNT network should be sufficiently strong. In view of this, the mechanical rigidity percolation should be considered additionally to conductivity percolation. Generally, the rigidity percolation, corresponding to the sol–gel transition, is characterized by a threshold concentration c_m higher than c_c. According to rough estimations, $c_m \approx 1.6 c_c$ (Sahimi, 1998). Assuming that this correlation is valid for the studied system and that $c_c \approx 0.05$ wt %, one can obtain that $c_m \approx 0.08$ wt %. Note that this value is by one order of magnitude lower than the value $c_m \approx 1$ wt % estimated for LC-aerosil suspensions (Glushchenko et al., 1997). This might be caused by extremely high aspect ratio of CNT particles capable to form connected structures at so low concentrations.

In summary, the following mechanism is responsible for the effect of electro-optical memory. Initially, LC is homeotropically aligned and CNTs are well aggregated. Electric field application leads to homeotropic-to-planar reorientation and development of electro-hydrodynamic flows in the LC phase. These flows crush bulky CNT aggregates, thus opening way for formation of fine CNT network supporting the planar LC alignment after the turning off the electric field. This mechanism is effective in the limited range of CNT concentrations. On the one hand, c should be higher than rigidity percolation threshold c_m.

On the other hand, it should not be rather high to prevent high electric conductivity of a system which causes critical lowering of the actual voltage applied to suspension and its essential heating.

6. Conclusions

Combination of liquid crystals and carbon nanotubes gives a class of unique composites with fascinating electrical, optical, electro-optical, nonlinear optical and structural properties. The present chapter describes a number of new-found interesting features of these composite materials. In general, a strong correlation between structural, electrical and electro-optic characteristics of LC-CNTs composites is observed.

It is shown that the CNTs shunt double electric layers in the LC cells and, in this way, change essentially a spatial distribution of the electric field applied to the cells. This explains reduction of controlling voltage and response time of LC layers doped by CNTs.

Same as in other liquids and polymers, CNTs demonstrate percolation behavior in LC hosts. At concentration of CNTs $c<0.01$ wt % in the LC-CNTs composites, the nanotubes exist in the form of individual aggregates. The further increase of c results in connection of isolated aggregates and, finally, in formation of continuous network of CNTs permeating LC matrix. The formed CNT network radically increases conductivity of LC samples and changes conductivity mechanism. At $c<0.01$ wt % ionic conductivity, typical for neat LCs, prevails. At $0.01<c<0.4$ wt %, the ionic charge transport is essentially enhanced by a charge hopping transport associated with a CNTs' skeleton. At higher CNT concentration, the conductivity mechanism typical for highly connected CNTs fully dominates. This change in the charge transport mechanisms with the CNTs concentration results in decay of conductivity activation energy from ~10 kJ/mol to ~0 kJ/mol.

The LC-CNTs composites based on the LCs with $\Delta\varepsilon<0$ demonstrate effect of electro-optic memory. It is connected with a metastable alignment state of LC phase stabilized by the network of CNTs acting as a spatially distributed alignment surface. This effect suggests new operation mode for LC devices and can be employed in the systems of information displaying and storage.

It is shown that the electrohydrodynamic flows developing in the LC phases may essentially influence structure of CNTs. Specifically, they crush aggregates of CNTs promoting formation of their finer structure. This suggests a unique method for in situ dispergation of CNTs in LCs. It is especially important for the CNTs non-grafted with special hydrophobic fragments facilitating dispergation of CNTs inside the LC matrix.

We strongly believe that the next studies will open new marvelous effects in these composites and their intriguing applications. Among the problems worthy of future investigation is influence of CNTs on the specific properties of LC materials, such as electrical, optical, thermal and mechanical anisotropy, molecular ordering and variety of phase transitions. It would be interesting to study fundamentally the peculiarities of structuring and percolation of CNTs in mesophases of different symmetry and origin, in the areas of phase transitions. Finally, it is worthwhile to investigate composites based on nanotubes with unusual properties and structure intensively generated by modern nanoscience and nanotechnology.

Acknowledgements

These studies were supported by European Social Fund grant GLOFY0102J, NAS of Ukraine (grant 10-07-H) and "Dnipro" program of Ukrainian-French scientific cooperation (grant M/16-2009).

7. References

Bahr, J. L.; Yang, J.; Kosynkin, D. V.; Bronikowski, M. J.; Smalley, R. E. & Tour, J. M. (2001). Functionalization of carbon nanotubes by electrochemical reduction of aryl diazonium salts: a bucky paper electrode. *J. Am. Chem. Soc.*, Vol. 123, No. 27, June 2001, pp. 6536-6542, DOI: 10.1021/ja010462s.

Baik, In-Su; Jeon, Sang Youn; Lee, Seung Hee; Park, K. Ah; Jeong S. H.; An, K. H. & Lee, Y. H. (2005). Electrical-field effect on carbon nanotubes in a twisted nematic liquid crystal cell. *Appl. Phys. Lett.*, Vol. 87, No. 26, December 2005, pp. (263110-1)-(263110-3), DOI: 10.1063/1.2158509.

Baik, In-Su; Jeon, S. Y.; Jeong, S. J.; Lee, S. H.; An, K. H.; Jeong, S. H. & Lee, Y. H. (2006). Local deformation of liquid crystal director induced by translational motion of carbon nanotubes under in-plane field. *J. Appl. Phys.*, Vol. 100, No. 7, October 2006, pp. (074306-1)-(074306-5), DOI: 10.1063/1.2355535.

Balberg, I.; Anderson, C. H.; Alexander, S.; & Wagner, N. (1984). Excluded volume and its relation to the onset of percolation. *Phys. Rev. B*, Vol. 30, No. 7, October 1984, pp. 3933–3943, DOI: 10.1103/PhysRevB.30.3933.

Barbero, G. & Olivero, D. (2002). Ions and nematic surface energy: belong the exponential approximation for the electric field of ionic origin. *Phys. Rev. E*, Vol. 65, February 2002, pp. (031701-1)-(031701-5), DOI: 10.1103/PhysRevE.65.031701.

Barrau, S.; Demont, P.; Peigney, A.; Laurent, C. & Lacabanne C. (2003). DC and AC conductivity of carbon nanotubes-polyepoxy composites. *Macromolecules*, Vol. 36, Iss. 14, June 2003, pp. 5187-5194, DOI: 10.1021/ma021263b.

Basu, R. & Iannacchione, G. S. (2008). Carbon nanotube dispersed liquid crystal: A nano electromechanical system. *Appl. Phys. Lett.*, Vol. 93, No. 18, November 2008, pp. (183105-1)-(183105-3), DOI: 10.1063/1.3005590.

Behnam, A.; Guo, J. & Urala, A. (2007). Effects of nanotube alignment and measurement direction on percolation resistivity in single-walled carbon nanotube films. *J. Appl. Phys.*, Vol. 102, Iss. 4, August 2007, pp. (044313-1)-(044313-7), DOI: 10.1063/1.2769953.

Belotskii, E. D.; Lev, B. I. & Tomchuk, P. M. (1980). Effective ion mass in a liquid crystal. *JETP Lett.*, Vol. 31, No. 10, May 1980, pp. 539-541.

Blinov, L. M. & Chigrinov, V. G. (1996). *Electrooptic Effects in Liquid Crystal Material*, Springer, ISBN: 0387947086, 9780387947082, New York.

Cervini, R.; Simon, G.; Ginic-Markovic, M.; Matisons, J.; Huynh, C. & Hawkins, S. (2008). Aligned silane-treated MWCNT/liquid crystal polymer films. *Nanotechnology*, Vol. 19, March 2008, pp. (175602-1)-(175602-10), DOI: 10.1088/0957-4484/19/17/175602.

Chelidze, T.L.; Derevyanko, A. I. & Kurilenko, O. D. (1977). *Electric Spectroscopy of Heterogeneous Systems*, Naukova Dumka, Kiev (in russian).

Chen, H-Y. & Lee W. (2006). Suppression of field screening in nematic liquid crystals by carbon nanotubes. *Appl. Phys. Lett.*, Vol. 88, No. 22, May 2006, pp. (222105-1)-(222105-3), DOI: 10.1063/1.2208373.

Chen, H-Y.; Lee, W. & Clark, N. A. (2007). Faster electro-optical response characteristics of a carbon-nanotube-nematic suspension. *Appl. Phys. Lett.*, Vol. 90, No. 3, January 2007, pp. (033510-1)-(033510-3), DOI: 10.1063/1.2432294.

Chen, Y-N.; Wu, J-J. & Ke H-L. (2008a). The Transverse Motions of Charged Nano-Particles under an AC Electric Field in a Nematic Liquid Crystal Cell. *Jap. J. Appl. Phys.*,Vol. 47, 8631–8634.

Chen, Yi Ning; Wu, Jin-Jei & Ke, Hung-Lin (2008b). Electrohydrodynamic behaviors in the multiwalled carbon nanotubes doped optically compensated bend polymer-dispersed nematic liquid crystal cell. *Jpn. J. Appl. Phys.*, Vol. 47, No. 11, July 2008, pp. 8487-8490, DOI: 10.1143/JJAP.47.8487.

Craig D.Q.M. (1995). *Dielectric Analysis of Pharmaceutical Systems*, Taylor & Francis Ltd., ISBN: 0-203-30257-5, 0-13-210279-X, London.

Dierking, I.; Scalia, G.; Morales, P. & LeClere, D. (2004). Aligning and Reorienting Carbon Nanotubes with Nematic Liquid Crystals. *Adv. Mat.*, Vol. 16, No. 11, June 2004, pp. 865-869, DOI: 10.1002/adma.200306196.

Dierking, I.; Casson, K. & Hampson R. (2008). Reorientation Dynamics of Liquid Crystal–Nanotube Dispersions. *Jpn. J. Appl. Phys.*,Vol. 47, April 2008, pp. 6390–6393, DOI: 10.1143/JJAP.47.6390.

Dolgov, L.; Yaroshchuk, O. & Lebovka, M. (2008). Effect of electro-optical memory in liquid crystals doped with carbon nanotubes. *Mol. Cryst. Liq. Cryst.*, Vol. 496, January 2008, pp. 212-229, ISSN: 1542-1406, DOI: 10.1080/15421400802451816.

Dolgov, L.; Lebovka, N. & Yaroshchuk, O. (2009). Effect of electrooptical memory in suspensions of carbon nanotubes in liquid crystals. *Colloid. J.*, Vol. 71, No. 5, August 2008, pp. 603-611, DOI: 10.1134/S1061933X09050044.

Du, F.; Fischer, J. E. & Winey, K. I. (2005). Effect of nanotube alignment on percolation conductivity in carbon nanotube/polymer composites. *Phys. Rev. B*, Vol. 72, September 2005, pp. (121404-1)-(121404-4), DOI: 10.1103/PhysRevB.72.121404.

Eletskii, A. V. (2009). Transport properties of carbon nanotubes. *Phys. Usp.*, Vol. 52, No. 3, March 2009, pp. 209-224, DOI: 10.3367/UFNe.0179.200903a.0225.

Foygel, M.; Morris, R. D.; Anez, D.; French, S. & Sobolev V. L. (2005). Theoretical and computational studies of carbon nanotube composites and suspensions: Electrical and thermal conductivity. Phys. Rev. B, Vol. 71, March 2005, pp. (104201-1)-(104201-6), DOI: 10.1103/PhysRevB.71.104201.

Frenkel, J. (1955). Kinetic Theory of Liquids. Dover, New York.

Gantmaher, V. F. (2005). *Electrons in disordered matters*. Fizmatlit, ISBN : 5-9221-0578-7, Moscow (in russian).

Giordani, S.; Bergin, S.; Nicolosi, V.; Lebedkin, S.; Kappes, M.; Blau, W. & Coleman, J. (2006) Debundling of single-wall nanotubes by dilution: observation of large populations of individual nanotubes in amide solvent dispersions. *J. Phys. Chem. B*, Vol. 110, No. 32, July 2006, pp. 15708-15718, DOI: 10.1021/jp0626216.

Glushchenko, A.; Kresse, H.; Reshetnyak, V.; Reznikov, Yu. & Yaroshchuk, O. (1997). Memory effect in filled nematic liquid crystals. *Liq. Cryst.*,Vol. 23, No. 2, March 1997, pp. 241-246.

Goncharuk, A. I.; Lebovka, N. I.; Lisetski L. N. & Minenko S. S. (2009). Aggregation, percolation and phase transitions in nematic liquid crystal EBBA doped with carbon nanotubes. *J. Phys. D : Appl. Phys.*, Vol. 42, July 2009, pp. (165411-1)-(165411-8), DOI: 10.1088/0022-3727/42/16/165411.

Grossiord, N.; Loos, J.; Regev, O. & Koning, C. E. (2006). Toolbox for dispersing carbon nanotubes into polymers to get conductive nanocomposites. *Chem. Mater.* Vol. 18, January 2006, pp. 1089–1099, DOI: 10.1021/cm051881h.

Haase, W. & Wrobel, S. (2003). *Relaxation Phenomena: liquid crystals, magnetic systems, polymers, high-tc superconductors, metallic glasses,* Springer, ISBN: 3540442693, Berlin Heidelberg New York.

Huang, C-Y.; Hu, C-Y.; Pan, H-C. & Lo K-Y. (2005). Electrooptical Responses of Carbon Nanotube-Doped Liquid Crystal Devices. *Jpn. J. Appl. Phys.*, Vol. 44, No. 11, November 2005, pp. 8077-8081, DOI: 10.1143/JJAP.44.8077.

Huang, C-Y. & Pan, H-C. (2006). Comment on "Electric-field effect on carbon nanotubes in a twisted nematic liquid crystal cell" [Appl. Phys. Lett. 87, 263110 (2005)] *Appl. Phys. Lett.*, Vol. 89, No. 5, July 2006, pp. (056101-1)-(056101-2), DOI: 10.1063/1.2243544.

Jager, K. M.; McQueen, D. H.; Tchmutin, I. A.; Ryvkina, N. G. & Kluppel, M. (2001). Electron transport and ac electrical properties of carbon black polymer composites. *J. Phys. D: Appl. Phys.*, Vol. 34, Iss. 17, August 2001, pp. 2699- 2707, DOI: 10.1088/0022-3727/34/17/319.

Jagota, A.; Diner, B.A.; Boussaad, S. & Zheng, M. (2005). Carbon nanotube—biomolecule interactions: Applications in carbon nanotube separation and biosensing, In: *Applied Physics of Carbon Nanotubes. Fundamentals of Theory, Optics and Transport Devices*, Rotkin, S. V. & Subramoney S., (Ed.), pp. 253-271, Springer, ISBN: 978-3-540-23110-3, Berlin-Heidelberg.

Jayalakshmi, V. & Prasad, S. K. (2009). Understanding the observation of large electrical conductivity in liquid crystal-carbon nanotube composites. *Appl. Phys. Lett.* Vol. 94, May 2009, pp. (202106-1)-(202106-3), DOI: 10.1063/1.3133352.

Jeong, S. J.; Park, K. A.; Jeong, S. H.; Jeong, H. J.; An, K. H.; Nah, C. W.; Pribat, D.; Lee, S. H. & Lee, Y. H. (2007). Electroactive superelongation of carbon nanotube aggregates in liquid crystal medium. *Nano Lett.*, Vol. 7, May 2007, pp. 2178-2182, DOI: 10.1021/nl070116u.

Johner, N.; Ryser, P.; Grimaldi, C. & Balberg, I. (2007). Piezoresistivity and tunneling-percolation transport in apparently nonuniversal systems. *Phys. Rev. B*, Vol. 75, Iss. 10, March 2007, pp. 104204-1)-(104204-9), DOI: 10.1103/PhysRevB.75.104204.

Johner, N.; Grimaldi, C.; Balberg, I. & Ryser, P. (2008). Transport exponent in a three-dimensional continuum tunneling-percolation model, *Phys. Rev. B*, Vol. 77, Iss. 17, May 2008, pp. (174204-1)-(174204-11), DOI: 10.1103/PhysRevB.77.174204.

Kim, B. K.; Lee, J. & Yu, I. (2003). Electrical properties of single-wall carbon nanotube and epoxy composites. *J. Appl. Phys.*, Vol. 94, Iss. 10, November 2003, pp. 6724-6728, DOI: 10.1063/1.1622772.

Koval'chuk, A. V. (1998). Low-frequency spectroscopy as an investigation method of the electrode-liquid interface. *Functional Materials*, Vol. 5, No. 3, pp. 426-430.

Koval'chuk, A.V. (2000). Mechanism of charge exchange at the liquid crystal-electrode interface. *JETP Lett.*, Vol. 72, No. 7, October 2000, pp. 377-380, DOI: 10.1134/1.1331150.

Koval'chuk, A. V.; Zakrevska, S. S.; Yaroshchuk, O. V. & Maschke, U. (2001a). Electrooptical properties of three-component compositions "liquid crystal-aerosil-photopolymer" *Mol. Cryst. Liq. Cryst.*, Vol. 368, August 2001, pp. 129-136, DOI: 10.1080/10587250108029939.

Koval'chuk, A. V. (2001b). Relaxation processes and charge transport across liquid crystal – electrode interface. *J. Phys.: Condens. Matter*, Vol. 13, November 2001, pp. 10333-10345, DOI: 101088/0953-8984/13/46/306.

Koval'chuk, A.V. (2001c). Low-frequecy dielectric relaxation at the tunnel charge transfer across the liquid/electrode interface. *Functional Materials*, Vol. 8, No. 4, October 2001, pp. 690-693.

Koval'chuk, A.V.; Dolgov, L. & Yaroshchuk O. (2008). Dielectric studies of dispersions of carbon nanotubes in liquid crystals 5CB. *Semiconductor Physics, Quantum Electronics & Optoelectronics*, Vol. 11, pp. 337-341.

Kreuzer, M.; Tschudi, T.; Eidenschink, R. (1992). Erasable optical storage in bistable liquid crystal cells. *Mol. Cryst. Liq. Cryst.*, Vol. 223, January 1992, pp. 219-227, DOI: 10.1080/15421409208048253.

Kyrylyuk, A. V. & van der Schoot P. (2008). Continuum percolation of carbon nanotubes in polymeric and colloidal media. *PNAS*, Vol. 105, No. 24, June 2008, pp. 8221–8226, DOI: 10.1073/pnas.0711449105.

Lagerwall, J. P. F.; Scalia, G.; Haluska, M.; Dettlaff-Weglikowska, U.; Giesselmann1, F. & Roth, S. (2006). Simultaneous alignment and dispersion of carbon nanotubes with lyotropic liquid crystals. *Phys. Stat. Sol. (b)*, Vol. 243, No. 13, August 2006, pp. 3046–3049, DOI: 10.1002/pssb.200669146.

Lagerwall, J. P. F.; Dabrowski, R. & Scalia, G. (2007). Antiferroelectric liquid crystals with induced intermediate polar phases and the effects of doping with carbon nanotubes. *J. Non-Cryst. Solids*, Vol. 353, October 2007, pp. 4411–4417, DOI: 10.1016/j.jnoncrysol.2007.01.094.

Lagerwall, J. & Scalia, G. (2008). Carbon nanotubes in liquid crystals. *J. Mater. Chemistry*, Vol. 18, Iss. 25, July 2008, pp. 2890–2898. DOI: 10.1039/b802707b.

Lebovka, N. I.; Manna, S. S.; Tarafdar, S. & Teslenko, N. (2002). Percolation in Models of Thin Film Depositions. *Phys. Rev. E*, Vol. 66, Iss. 6, December 2002, pp. (066134-1)-(1066134-4), DOI: 10.1103/PhysRevE.66.066134.

Lebovka, N.; Dadakova, T.; Lysetskiy, L.; Melezhyk, O.; Puchkovska, G.; Gavrilko, T.; Baran, J. & Drozd, M. (2008). Phase transitions, intermolecular interactions and electrical conductivity behavior in carbon multiwalled nanotubes/nematic liquid crystal composites. *J. Mol. Struct.*, Vol. 877, Iss. 1-3, January 2008, pp. 135-143, DOI: 10.1016/j.molstruc.2007.12.038.

Lebovka, N. I.; Goncharuk, A.; Melnyk, V.I. & Puchkovska G.A. (2009). Interface interactions in benzophenone doped by multiwalled carbon nanotubes. *Physica E*, Vol. 41, Iss. 8, August 2009, pp. 1554–1560, DOI: 10.1016/j.physe.2009.04.038.

Lee, W.; Wang, Chun-Yu & Shih, Yu-Cheng. (2004). Effects of carbon nanosolids on the electro-optical properties of a twisted nematic liquid-crystal host. *Appl. Phys. Lett.*, Vol. 85, No. 4, July 2004, pp. 513-515, DOI: 10.1063/1.1771799.

Lee, W.; Chen, H –Y. & Shih, Y-C. (2008). Reduced dc offset and faster dynamic response in a carbon-nanotube-impregnated liquid-crystal display. *J. Soc. Info. Display*, Vol. 16, No. 7, May 2008, pp. 733-741, DOI:10.1889/1.2953480.

Licristal® (2002). Liquid crystal mixtures for electro-optic displays catalogue. Merck KGaA, Darmstadt, Germany.

Lisetski, L. N.; Lebovka, N. I.; Sidletskiy, O. Ts.; Panikarskaya, V. D.; Kasian, N. A.; Kositsyn, S. S.; Lisunova, M. O. & Melezhyk, O. V. (2007). Spectrophotometry and electrical conductivity studies of multiwalled dispersed in nematic liquid crystals. *Functional Materials*, Vol. 14, No. 2, January 2007, pp. 233-237.

Lisetski, L. N.; Minenko, S. S.; Fedoryako, A. P. & Lebovka, N. I. (2009). Dispersions of multiwalled carbon nanotubes in different nematic mesogens: The study of optical transmittance and electrical conductivity, *Physica E*, Vol. 41, Iss. 3, October 2008, pp. 431-435, DOI: 10.1016/j.physe.2008.09.004.

Lisunova, M. O., Mamunya, Ye. P. ; Lebovka, N. I. & Melezhyk, A. V. (2007). Percolation behaviour of ultrahigh molecular weight polyethylene/multi-walled carbon nanotubes composites. *Eur. Pol. J.*, Vol. 43, Iss. 3, March 2007, pp. 949-958, DOI: 10.1016/j.europolymj.2006.12.015.

Liu, J.; Casavant, M. J.; Cox, M.; Walters, D. A.; Boul, P.; Lu, W.; Rimberg, A. J.; Smith, K. A.; Coldert, D. T. & Smalley, R. E. (1999). Controlled deposition of individual single-walled carbon nanotubes on chemically functionalized templates. *Chem. Phys. Lett.* Vol. 303, No. 1-2, April 1999, pp. 125-129, DOI: 10.1016/S0009-2614(99)00209-2.

Liu, L.; Matitsine, S.; Gan, Y. B.; Chen, L. F.; Kong, L. B. & Rozanov, K. N. (2007). Frequency dependence of effective permittivity of carbon nanotube composites. *J. Appl. Phys.*, Vol. 101, Iss. 9, May 2007, pp. (094106-1)-(094106-6), DOI: 10.1063/1.2728765.

Lu, S.-Y. & Chien, L.-C. (2008). Carbon nanotube doped liquid crystal OCB cells: Dielectric and electro-optical properties. *Digest of Technical Papers - SID International Symposium*, Vol. 39, Iss. 3, 1853-1856.

Lynch, M. D. & Patrick, D. L. (2002). Organizing carbon nanotubes with liquid crystal solvents. *Nano Lett.*, Vol. 2, No. 11, September 2002, pp. 1197–1201, DOI: 10.1021/nl025694j.

Mamunya, Ye. P. ; Lebovka, N. I.; Lisunova, M. O.; Lebedev, E. V. & Boiteux, G. (2008). Conductive polymer composites with ultralow percolation threshold containing carbon nanotubes. *J. Nanostruct. Pol. & Nanocompos.*, Vol. 4, Iss. 1, January 2008, pp. 21-27, ISSN: 1790-4439.

Mdarhri, A.; Carmona, F.; Brosseau, C. & Delhaes, P. (2008). Direct current electrical and microwave properties of polymer-multiwalled carbon nanotubes composites. *J. Appl. Phys.*, Vol. 103, Iss. 5, March 2008, pp. (054303-1)-(054303-9), DOI: 10.1063/1.2841461.

Melezhyk, A. V., Sementsov, Yu. I. & Yanchenko V. V. (2005). Synthesis of porous carbon nanofibers on catalysts fabricated by the mechanochemical method. *Rus. J. Appl. Chem.*, Vol. 78, No. 6, August 2005, pp. 924–930, DOI: 10.1007/s11167-005-0421-x.

Mott, N. F. & Davis, E.A. (1971). *Electronic processes in Non-Crystalline Materials*, Clarendon Press, ISBN: 0198512597, Oxford.

Muller, K.-H.; Wei, G.; Raguse, B. & Myers, J. (2003). Three-dimensional percolation effect on electrical conductivity in films of metal nanoparticles linked by organic molecules. *Phys. Rev. B*, Vol. 68, Iss. 15, October 2003, pp. (155407-1)-(155407-6), DOI: 10.1103/PhysRevB.68.155407.

Pike, G. E. (1972). ac Conductivity of scandium oxide and a new hopping model for conductivity. *Phys Rev. B*, Vol. 6, Iss. 4, January 1972, pp. 1572-1580, DOI: 10.1103/PhysRevB.6.1572.

Podgornov, F. V.; Suvorova, A. M.; Lapanik, A. V. & Haase, W. (2009). Electrooptic and dielectric properties of ferroelectric liquid crystal/single walled carbon nanotubes dispersions confined in thin cells. *Chem. Phys. Lett.*, Vol. 479, Iss. 4-6, August 2009, pp. 206-210, DOI: 10.1016/j.cplett.2009.08.005.

Prakash, J.; Choudhary, A.; Mehta, D. S. & Biradar A. M. (2009). Effect of carbon nanotubes on response time of ferroelectric liquid crystals. *Phys. Rev. E*, Vol. 80, Iss. 1, July 2009, pp. (012701-1)-(012701-4), DOI: 10.1103/PhysRevE.80.012701.

Qi, H. & Hegmann, T. (2008). Impact of nanoscale particles and carbon nanotubes on current and future generations of liquid crystal displays. *J. Mater. Chem.*, Vol. 18, No. 28, July 2008, pp. 3288 - 3294, DOI: 10.1039/b718920f.

Rahman, M. & Lee, W. (2009). Scientific duo of carbon nanotubes and nematic liquid crystals. *J. Phys. D: Appl. Phys.*, Vol. 42, No. 6, January 2009, pp. (063001-1)-(063001-12), DOI: 10.1088/0022-3727/42/6/063001.

Sahimi, M. (1998). Non-linear and non-local transport processes in heterogeneous media: from long-range correlated percolation to fracture and materials breakdown. *Phys. Rep.*, Vol. 306, Iss. 4-6, November 1998, pp. 213-395, DOI: 10.1016/S0370-1573(98)00024-6.

Shah, H. J.; Fontecchio, A. K.; Mattia, D. & Gogotsi, Yu. (2008). Field controlled nematic-to-isotropic phase transition in liquid crystal-carbon nanotube composite. *J. Appl. Phys.*, Vol. 103, December 2007, pp. (064314-1)-(064314-5), DOI: 10.1063/1.2844384.

Shklovskii, B.I. & Efros, A. L. (1984). *Electronic Properties of Doped Semiconductors*, Springer Series in Solid-State Sciences, Vol. 45, Springer-Verlag, ISBN: 0387129952, Berlin.

Stauffer, D. & Aharony, A. (1992). *Introduction to Percolation Theory*, Taylor & Francis, ISBN: 0748402535, London.

Straley, J. P. (1977). Critical exponents for the conductivity of random resistor lattices. *Phys. Rev. B*, Vol. 15, Iss. 12, June 1977, pp. 5733 -5737, DOI : 10.1103/PhysRevB.15.5733.

Torquato, S (2002). *Random Heterogeneous Materials: Microstructure and Macroscopic Properties*, Springer, ISBN: 0-387-95167-9, New York.

Trushkevych, O.; Collings, N.; Hasan, T.; Scardaci, V.; Ferrari, A. C.; Wilkinson, T. D.; Crossland, W. A.; Milne, W. I.; Geng, J.; Johnson, B. F. G. & Macaulay, S. (2008). Characterization of carbon nanotube–thermotropic nematic liquid crystal composites. *J. Phys. D: Appl. Phys.*, Vol. 41, May 2008, pp. (125106-1)-(125106-11), DOI: 10.1088/0022-3727/41/12/125106.

Twarowski, A. J. & Albrecht, A. C. (1979). Depletion layer in organic films: Low frequency measurements in polycrystalline tetracene. *J. Chem. Phys.* Vol. 20, No. 5, March 1979, pp. 2255-2261, DOI: 10.1063/1.437729.

Weiss, V.; Thiruvengadathan, R. & Regev, O. (2006). Preparation and characterization of a carbon nanotube-lyotropic liquid crystal composite. *Langmuir*, Vol. 22, No. 3, November 2005, pp. 854-856, DOI: 10.1021/la052746m.

Yaroshchuk, O.; Koval'chuk, O. & Kravchuk, R. (2005). The interfacial dipole-to-dipole interaction as a factor of polar anchoring in the cells with planar liquid crystal alignment. *Mol. Gryst. Liq. Cryst.*, Vol. 438, June 2005, pp. 195/[1759] - 204/[1768], DOI: 10.1080/15421400590958151.

Yaroshchuk, O.; Tomylko, S.; Dolgov, L.; Semikina, T. & Kovalchuk, O. (2010). Carbon nanotubes doped liquid crystals: robust composites with a function of electro-optic memory. *Diamond & Related Materials*. In print. DOI:10.1016/j.diamond.2010.01.022

Zhao, W.; Wang, J.; He, J.; Zhang, L.; Wang, X. & Li, R. (2009). Preparation and characterization of carbon nanotubes/monotropic liquid crystal composites. Appl. Surface Sci., Vol. 255, Iss. 13-14, April 2009, pp. 6589-6592, DOI: 10.1016/j.apsusc.2009.02.048.

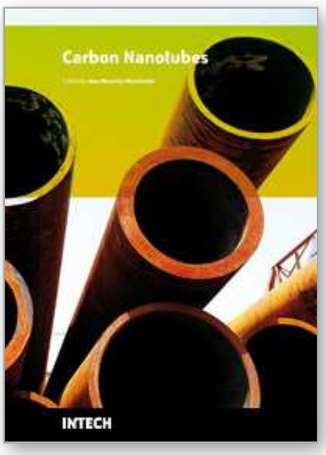

Carbon Nanotubes

Edited by Jose Mauricio Marulanda

ISBN 978-953-307-054-4
Hard cover, 766 pages
Publisher InTech
Published online 01, March, 2010
Published in print edition March, 2010

This book has been outlined as follows: A review on the literature and increasing research interests in the field of carbon nanotubes. Fabrication techniques followed by an analysis on the physical properties of carbon nanotubes. The device physics of implemented carbon nanotubes applications along with proposed models in an effort to describe their behavior in circuits and interconnects. And ultimately, the book pursues a significant amount of work in applications of carbon nanotubes in sensors, nanoparticles and nanostructures, and biotechnology. Readers of this book should have a strong background on physical electronics and semiconductor device physics. Philanthropists and readers with strong background in quantum transport physics and semiconductors materials could definitely benefit from the results presented in the chapters of this book. Especially, those with research interests in the areas of nanoparticles and nanotechnology.

INTECH
open science | open minds

InTech Europe
University Campus STeP Ri
Slavka Krautzeka 83/A
51000 Rijeka, Croatia
Phone: +385 (51) 770 447
Fax: +385 (51) 686 166
www.intechopen.com

InTech China
Unit 405, Office Block, Hotel Equatorial Shanghai
No.65, Yan An Road (West), Shanghai, 200040, China
中国上海市延安西路65号上海国际贵都大饭店办公楼405单元
Phone: +86-21-62489820
Fax: +86-21-62489821

IntechOpen